2011

The Presentation and Perception of Virtual Textures through a Haptic Matrix Display Device

Patrick Headley
Virginia Commonwealth University

The Presentation and Perception of Virtual Textures through a Haptic Matrix Display Device

A thesis submitted in partial fulfillment of the requirements for the degree of Master of Science at Virginia Commonwealth University.

by

Patrick Christopher Headley
Bachelor of Science
Virginia Commonwealth University, 2009

Director: Dr. Dianne T.V. Pawluk
Assistant Professor, Department of Biomedical Engineering

Virginia Commonwealth University
Richmond, Virginia
May 2011

Acknowledgement

I would like to thank my loving wife, Lauren, for her constant support and patience over the past two years and beyond. I would not be the person I am today without her. I would also like to thank my family, especially my loving parents, and friends who have also supported me and continually expressed interest in my work. The members of the Haptics Laboratory, David, Ravi, Justin, Ketan, Devnath, and Vicky, have all been an invaluable resource as well as good friends. Finally, I would like to thank Dr. Pawluk for her guidance and mentorship on this project, and for being so generous with her time.

Table of Contents

List of Tables

List of Figures

Abstract

THE PRESENTATION AND PERCEPTION OF VIRTUAL TEXTURES THROUGH A HAPTIC MATRIX DISPLAY DEVICE

By Patrick Christopher Headley, BS Biomedical Engineering

A thesis submitted in partial fulfillment of the requirements for the degree of Master of Science at Virginia Commonwealth University.

Virginia Commonwealth University, 2011

Director: Dr. Dianne T.V. Pawluk
Assistant Professor, Department of Biomedical Engineering

Dynamic, refreshable tactile displays offer a method of displaying graphical information to people who are blind or visually impaired. Texture, which is already used as an effective method to present graphical information in physical tactile diagrams, conceivably constitutes the best way to present graphics through a tactile display. This thesis presents the design of a new low-cost haptic matrix display device capable of displaying graphical information through virtual textures. The perception of virtual textures through the display is examined through three main experiments. The first two experiments examine the perception of square wave gratings through the device. The final experiment examines the effect of texture adaptation when using the device, and compares it to exploration with a handheld probe and the bare finger. The results show that haptic matrix displays can be used to display graphical information through texture and offer guidelines in the production of such textures.

1. Introduction

Most information in our world is presented to be accessed in a visual format. Unfortunately, for people who are blind or visually impaired, this format is inaccessible, or very difficult to use depending on the degree of impairment. Fortunately, text information can be easily translated to other formats such as through text-to-speech programs or text-to-electronic Braille display programs. However, graphical information is much more difficult to access. This is problematic as visual graphical formats are increasingly becoming the sole source of information, whether for accessing information from the internet, describing concepts in textbooks, workplace presentations, and so forth. Although there exist methods and services to allow visually impaired people to access graphical information, they have drawbacks. Custom-made graphs and maps constructed from various textured materials (known as tactile experience pictures), swell-paper raised line drawings, and even mass-produced Thermoform tactile graphics are usually time-consuming and expensive to make (Vidal-Verdu and Hafez, 2007). Furthermore, these materials are bulky and awkward to transport and store, can deteriorate with time, and are static – that is, they can only display one graphic.

Refreshable tactile displays provide an alternative that is easy to reproduce, transport and store, and can represent many different graphics in rapid succession. However, they have tended to focus on the portrayal of raised outlines, which, even for common objects, prove difficult to interpret (Loomis, Klatzky, and Lederman 1991). In contrast, tactile experience pictures, which represent objects and object parts by a variety of physical materials and textures, are easily interpreted even by young children. This is likely because the human haptic system is particularly adept at processing textural information, making diagrams composed of textured material, such as tactile experience pictures, very salient. These different physical materials are

also used in other hand-made graphics, such as for geographical diagrams and other such illustrations. Texture has also been used in the TexyForm system to design tactile pictures and was found to improve performance significantly (Thompson, Chronicle, and Collins, 2006). The use of texture in tactile displays has the potential to improve the usability of these devices by taking advantage of the strengths of the human haptic system.

Texture and texture perception is also a very important topic in general for the study of haptics. The burgeoning study of haptics has widespread applications, including not only for tactile graphics for people with visual impairments, but also in a wide range of virtual reality applications, including gaming, simulation, and telemedicine. The simulation and virtual display of real textured surfaces can be used efficiently and effectively to identify components, such as different bodily tissues in telesurgery. Advancements in the knowledge of human texture perception and the display of virtual textures are needed to further these important fields.

The work presented here focuses on the presentation and perception of virtual textures on a haptic matrix display, developed specifically for the purpose of making visual graphical data normally displayed on a computer accessible in a tactile format. After the presentation of background information pertaining to visual impairment, the human haptic system and texture perception, the development of the display will be presented, from modifications made to the previous version of the device to the current version. Finally, several experiments are presented which help to determine the way in which texture is perceived through the haptic matrix display. The first two experiments examine how people perceive virtual square wave gratings (widely studied physical stimuli) through the display device. The results have important implications for the parameters which should be used in the construction of salient virtual textures. The last experiment examines whether the exploration of virtual textures with a matrix display device

will be hampered by adaptation to the textures themselves, a potential problem with the use of texture in tactile diagrams.

2. Background

This section will briefly touch on the differences in visual impairment before examining haptic displays, primarily tactile matrix displays. It will then introduce human haptics, reviewing the anatomy and neurophysiology of touch. Finally, the perception of textures via the bare finger and a handheld probe will be reviewed, as well as the effects of vibrotactile adaptation.

2.1 The Spectrum of Visual Impairment

Visual impairment can come in varying degrees, spanning from non-impaired vision to total blindness. Not only can visual impairment vary from low vision to legal blindness to only light perception to complete blindness, but age at onset and causes of visual impairment also vary widely. People who are born totally blind are said to be congenitally blind. If someone becomes blind later in life, he or she is said to be adventitiously blind. The causes of visual impairment and blindness are also many and varied. Glaucoma and macular degeneration are among the leading causes. Cataract, diabetic retinopathy, retinitis pigmentosa, and optic nerve atrophy also cause visual impairment or blindness. (Levesque 2005)

Sighted, congenitally blind and adventitiously blind persons have been shown on certain tasks to have different performance (e.g., Thompson, Chronicle, and Collins, 2006), but in other experiments have been shown to perform similarly (e.g., Heller 1989). Sighted and adventitiously blind persons may benefit from visual imagery, especially in the perception of tactile pictures. Alternatively, the tactile experience which comes from reading Braille may give blind persons a heightened sense of tactile sensing, again, at least on some tasks (e.g., Alary et al., 2009). Thus any investigation of texture perception should take into account the amount of visual impairment in participants.

Although the immediate motivation for our study was to understand how individuals who are visually impaired perceived texture on a matrix display, as they are our target population, sighted participants were included as well. There are two reasons for this: 1) blind participants can be difficult to recruit for the many tests involved in the development of a system and we were interested in knowing whether sighted individuals could be used during the design process, and 2) this device (and other tactile matrix display devices) may find application beyond the blind community. Thus, it was important for us to study both groups. Blind subjects were not further divided into different levels of vision, such as congenitally vs. adventitiously blind persons, due to the difficulty in recruiting blind subjects, congenitally blind subjects in particular.

2.2 Haptic Displays

There exist only a few commercially available haptic displays which tend to be very expensive, typically costing tens of thousands of dollars. Perhaps the most widely used is the PHANTOM line of force feedback devices (Sensable, Wilmington, MA). This device and other force-feedback devices like it present forces to the hand or finger depending on the position of a single point within a virtual region. This is likely very difficult to interpret. Haptic matrix displays provide more information through distributed information to the finger tip.

2.3 Dynamic, Refreshable Matrix Display Devices

Many dynamic and refreshable haptic matrix display devices have been conceived, prototyped, and researched at universities around the world (Vidal-Verdu and Hafez, 2007). Chan et al. (2007) developed a virtual haptic display consisting of several Braille cells mounted onto a moveable carriage. Rovira et al. (2010) have been developing and testing the Tactos system, in which the user explores a graphics tablet with a stylus in one hand while the other hand rests on a

box containing two Braille cells which respond to the stylus movement. Levesque and Hayward (2008) have also used their STReSS^2 tactile rendering system, which laterally deforms the skin, to display tactile graphics. However, only a few devices have actually been brought to market and distributed relatively widely.

The two known commercial devices have been the Optacon and the Virtouch mouse (both currently out of business). The Optacon, originally conceived by Linvill and Bliss (1966), was the earliest dynamic refreshable haptic display and consisted of a six–by-twenty-four matrix of vibrated pins at 250 Hz (Bliss et al. 1970). However, it was difficult to use (Craig 1977) which was likely due to the fact that it mainly excited receptors that have poor spatial resolution (i.e., the FAII units). The Virtouch Mouse, also known as the VT Player, consisted of two four-by-four pin arrays, and was the object of several studies (e.g., Wall and Brewster 2006; Thomas, Isabelle, and Benoit, 2006). However, it: (1) only had a bandwidth of 10 Hz, which is very limiting in displaying tactile information, much of which is dynamic, (2) a time delay of 200 msec, and (3) significant position inaccuracies by using an optical mouse. Rastogi et al. (2010) presented a modified VT Player, with an absolute positioning system and relocated position sensor concurrent with the placement of the tactile display elements. This greatly improved accuracy in a tactile perception task. The use of a graphics tablet and RF coil constitute the absolute positioning system.

2.3.1 Current Lab Matrix Device

A new haptic matrix display, based on Rastogi's modified VT Player, was built in the laboratory consisting of four main commercially-available components: a Braille cell (P16, Metec AG), a 200 V power supply (Metec AG), a digital I/O (National Instruments USB-6501), and a graphics tablet (currently an Adesso CyberTablet 12000). The Braille cell, which houses a

two-by-four pin array constituting the tactile interface of the device, is situated inside of a commercially-available mouse casing. As with normal use of a Braille cell, the pins are driven either to be fully up or fully down. Also contained in the mouse casing is a RF transmitter tuned to communicate absolute position information to the graphics tablet (see Owen et al. 2009). The coil of the transmitter is centered under the pin array of the Braille cell as specified by Rastogi et al. (2010). The digital I/O, power supply, and driving electronics are contained within an electronics module to which the mouse is connected via cable. Unlike normal Braille cells, the pins are driven in parallel – this greatly improves the bandwidth of the device and somewhat improves the time delay, over that of the VT Player. In addition, the device was developed for less than $400, an important consideration for users who are blind or visually impaired, most of whom live below the poverty line.

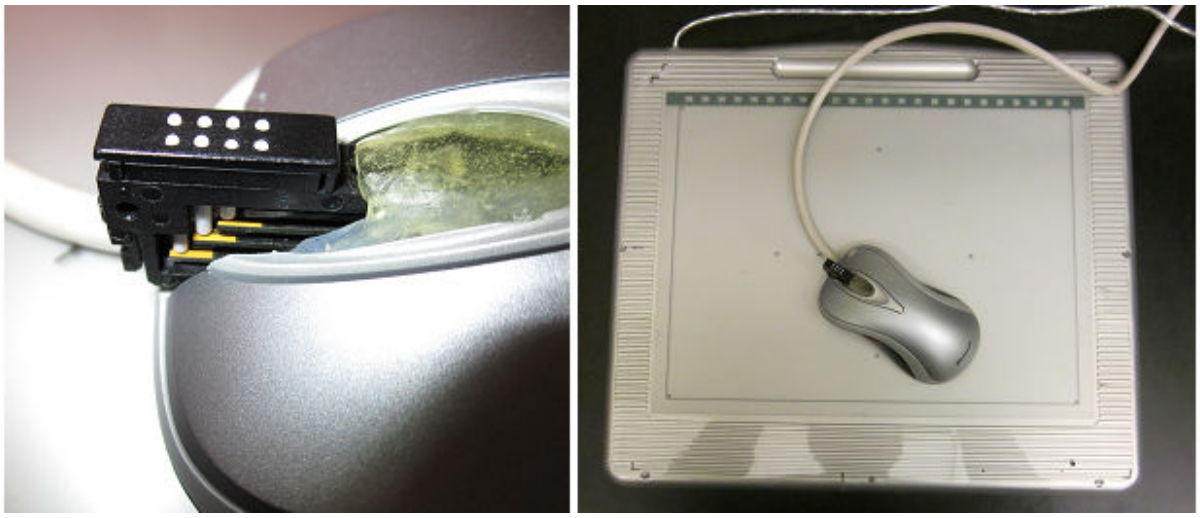

Figure 1. The haptic matrix display device close-up (left) and with the graphics tablet (right).

2.4 Haptics

2.4.1 Tactile Sense

Anatomy / Physiology of Touch

The surface of the hand is anatomically defined as having two surfaces, a dorsal surface and a volar surface. The skin of the volar, or palmar, aspect of the hand is called the glabrous or non-hairy skin. The skin of the fingerpad is stretched over the distal phalanx, the distal end of which is flattened into a tuft. Moving proximally, the distal phalanx articulates with the middle phalanx via the distal interphalangeal (DIP) joint (for the index, middle, ring, and little fingers; the thumb does not contain a middle phalanx). The proximal interphalangeal (PIP) joint connects the middle phalanx to the proximal phalanx, and the metacarpophalangeal (MP) joint connects the proximal phalanx to the metacarpal bone. Twenty-seven bones in total make up the hand and wrist. (Jones & Lederman, 2006)

The glabrous skin of the hand is thick, as compared to the thin skin on the dorsal aspect of the hand. Fibrillar tissue tethers the core layers of the dermis of the glabrous skin to flexor tendon sheaths, securing it in place. The dermis is covered by the epidermis; all skin is comprised of these two layers. However, several subdivisions exist. The epidermis of the glabrous skin of the fingerpad (and indeed of the whole hand) can be subdivided into five layers: the stratum corneum (the outermost layer), moving inward the stratum lucidum, the stratum granulosum, followed by the stratum spinosum, and finally the stratum germinativum. The cells of the epidermis are produced by subdivision at the stratum germinativum; during the course of about 28 days (for persons under 50 years of age) these cells migrate outward toward the stratum

corneum. As the cells migrate, they flatten, dehydrate, and fill with keratin. The cells of the stratum corneum slough off as they are constantly replaced. (Jones & Lederman, 2006)

The dermis is comprised of two layers, the papillary layer, which connects with the stratum germinativum of the epidermis via papillary folds, and the reticular layer. It is these papillary folds which are manifested on the fingerpad as fingerprints; these ridges can indeed be found on the entire volar surface of the hand. The dermis is much thicker than the epidermis (by a factor of 5-7) and accounts for 15-20% of the weight of the entire human body. Structurally, the dermis is an important component of the skin. It contains collagen, elastin, and reticular fibers which contribute to the mechanical properties of the glabrous skin. Collagen comprises about three-fourths of the dry weight of dermal skin; elastin accounts for 4% (Fung, 1993). The elastin is concentrated in the deeper layers of the dermis and provides the property of elasticity. The dermal layers of the skin also contain sweat glands and a dense vasculature which nourishes the adjacent epidermis. (Jones & Lederman, 2006)

Neurophysiology

Glabrous skin is known to contain at least four types of mechanoreceptors, and the human fingerpad is densely populated with these sensory organs. Merkel cells are found in the base of the epidermis, in the deep projections of the papillary folds. These mechanoreceptors respond to static touch and very low-frequency stimuli, and are associated with SA I (slowly adapting, see below) afferent nerve fibers. Meissner's corpuscles are located in the dermis, in the "peaks" of the papillary ridges. These respond to low-frequency vibrations ("flutter") and are associated with FA I (fast adapting, see below) afferents. Deeper into the dermis can be found Ruffini endings, which are spindle-shaped, respond to skin stretch, and are associated with SA II afferents. Finally, Pacinian corpuscles, associated with the FAII afferents, are contained in both

the basal layers of the dermis and the underlying subcutaneous fatty tissue. These large mechanoreceptors respond primarily to high frequency stimuli, for which they are very sensitive, but have large receptive fields. (Jones & Lederman, 2006)

The afferent nerve fiber types are named according to the nature of their neural impulse train in response to a ramp-and-hold stimulus and also according to the size of their receptive field (See Figure 2 below). FA I and FA II (fast adapting) fibers will respond to changes in the deformation of the surface of the skin, but will not respond to static deformation. SA I and SA II (slowly adapting) fibers, on the other hand, will continue to respond. FA I and SA I afferents have small receptive fields, which result in high spatial resolution, whereas FA II and SA II afferents have large receptive fields and thus low spatial resolution.

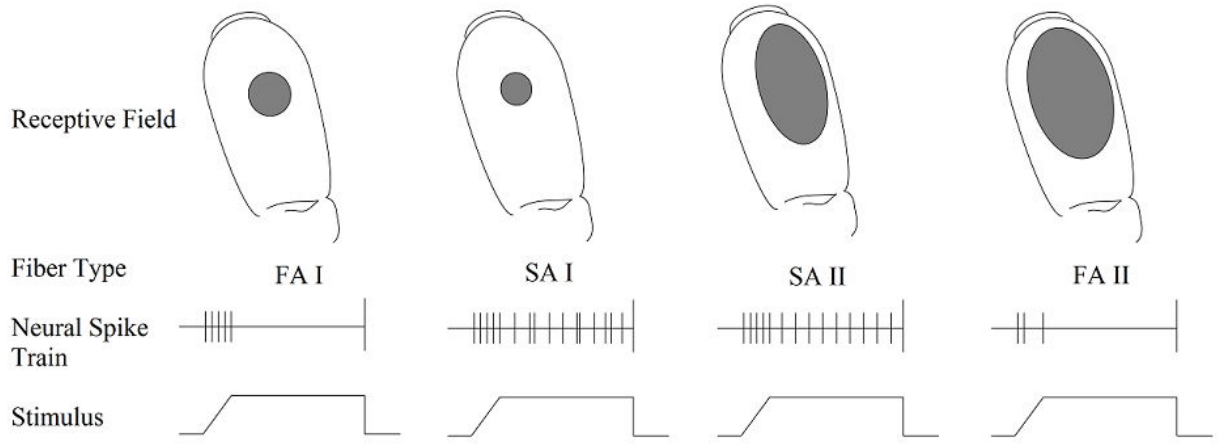

Figure 2. Receptive fields and neural spike trains of the nerve fibers in glabrous skin.

Channels of Touch

A hypothesis has been set forth which asserts that information-processing channels operate in the sense of touch mediated through the glabrous skin of the hand (Gescheider et al., 2009). These channels are linked to the four populations of mechanoreceptors reviewed above and are believed to operate independently. The conception of the multichannel theory of tactile

perception was based on experiments in which such factors as contactor size and frequency were varied, and adaptation was used in some cases, as described by Gescheider, Wright, and Verrillo (2009). The activation thresholds for each of the four channels change with stimulus frequency. At any given frequency, the channel with the lowest activation threshold will respond to the minimally-detectable stimulus. The channel with the lowest threshold changes as the stimulus frequency increases; thus different channels will respond to different threshold stimuli. High-frequency stimulation will primarily excite the Pacinian channel; low-frequency stimulation greater than about 2 Hz will primarily stimulate the FA I channel; static touch (very low frequencies) primarily stimulates the SA I channel. These thresholds are not fixed, however; adaptation to a stimulus of a certain frequency can raise the activation threshold of one channel to the point that another channel becomes the one with the lowest activation threshold at that frequency. Adaptation is further discussed below in Section 2.4.3.

It is important to note that the multichannel theory predicts that a stimulus that is above the activation thresholds of multiple channels will excite multiple channels. The stimuli we encounter daily are often complex and most likely activate multiple touch channels at any given time. The perception of complex textures, therefore, is likely mediated by several different channels of touch simultaneously.

2.4.2 Kinesthetic Sense

Included in the haptic sense is the sense of kinesthesia; that is, the sense of position. Although the kinesthetic receptors may play a role in the perception of texture through the device described in this work, its mechanisms are not explored in depth. At least for the perception of textures with a bare finger, the kinesthetic sense is not needed as the same results can be obtained with active and passive touch (Lederman 1981).

2.4.3 Texture Perception

The perception of texture has been studied extensively. In a study examining the perceptual dimensions of texture, Hollins et al. (1993) found roughness-smoothness to be the most readily apparent dimension, with hardness-softness following; ”stickiness” may constitute a third dimension. Appropriately, the most prominently studied dimension of texture in the literature, and the one that we focus on in this thesis, is the study of the perception of roughness. The perception of roughness by both the bare finger and a hand-held probe, whether real or virtual, has in turn been greatly studied. Both have some similarities to the mechanics of using a matrix array, as we have created. Similar to a bare finger, a matrix array of pins provides direct indentation of the finger (as opposed to a probe) and this information is distributed across the fingerpad. However, when a bare finger is used with a real surface, the form of the surface is continuous, whereas, with a matrix display it is crudely approximated by the spacing of the pins. The similarity with a probe is most apparent when considering a matrix of size one (i.e., one pin). In this case, the information can only be conveyed through the temporal response as with a probe. However, in contrast to the probe, the indentation response of the finger to the presented display is direct and spatially distributed.

Exploration with the bare finger

The exploration of physical square-wave gratings, one controlled form of texture, by the bare finger was studied by Lederman (e.g., 1974) and Lawrence et al. (2007). Both studies found that the perceived roughness increased as a function of increasing groove width over a significant range, up to a certain point at which the response flattens. Ridge width was found to be statistically significant but small in effect, causing a slight decrease in perceived roughness. Conner et al. (1990) used another form of controlled texture, a 2-D raised dot array where the

dots were constant in size, while the interelement spacing was varied. They found that perceived roughness was a quadratic inverted U-shaped function of interelement spacing when dot arrays are explored with the bare finger. Dot size, like ridge width, only had minor effects

Taylor and Lederman (1975) explained their results by describing roughness as a power function of the total area of the skin that is instantaneously deformed. Further observations by Conner et al. (1992) suggested that spatial coding by the afferent nerve fibers is involved, consistent with Taylor and Lederman's model. More specifically, they implicated the spatial coding by the slowly adapting type I receptors (SA Is) as involved in this process.

In contrast, Smith et al. (2002), who used non-rigid dot patterns with deep grooves, found that roughness estimates increased nearly linearly with spatial period up to 8.5 mm. They also found that roughness estimates are strongly predicted by temporal factors, namely, the rate of change in force in the scanning direction. They also suggested this change is coded by the FAI receptors.

More recently, the study of texture perception has shown different results depending on the fineness of the grating, separating stimuli into those having spatial periods greater than 0.2mm (macro-textures) and less than 0.2mm (micro-textures). Towards this end, Hollins (2000) has shown evidence supporting a duplex theory of texture perception, which states that the perception of micro-textures is mediated through channels of touch sensitive to vibration, while perception of macro-textures is mediated through channels sensitive to spatial deformation. Bensmaia and Hollins (2003) have implicated the FA II channel for perceiving micro-textures with the bare hand. They have proposed that it is increases in the power of the vibrations, weighted according to the spectral sensitivity of the FA II channel, which correlates with increases in roughness.

Exploration with a handheld probe

When a surface is explored with a handheld probe, the mechanoreceptors encode the shape of the probe itself; spatial cues of the surface being explored are no longer available. What is available is the perception of vibrations transmitted through the probe to the fingers. So we would expect some differences in the response to textures with a handheld probe than with a bare finger. However, as with the bare finger, the shape of the curve obtained when perceiving roughness through a handheld probe depends on the nature of the stimuli themselves. Lawrence et al. (2007) found that when the same square wave gratings used for the bare finger were explored with a handheld probe, perceived roughness also increased with increasing groove width from 0.125 mm to 2 mm and then stayed constant after 2 mm. Klatzky et al. (2003) examined perceived roughness when jittered raised dot patterns were explored with a probe and found the response to be an inverted U-shaped function of interelement spacing, which is akin to groove width as the dot size is constant.

Klatzky et al. (2003) found the response curves to also be sensitive to applied force, scanning velocity and probe diameter. They proposed that the peak of the roughness function could be predicted by the geometric interaction between the probe tip and stimuli elements; namely, the peak would occur when the interelement spacing was equal to the probe tip diameter – this spacing Klatzky has named the "drop point," as it is the point at which the probe will "drop" between stimuli elements. This would maximize the amplitude of vibrations as well as maximize the frequency at which the maximum amplitudes are felt.

Several studies have examined the perceptual response to the generation of virtual textures presented with a force-reflecting single point contact device. As this is a case of indirect touch, it is similar to the exploration of physical textures with a probe. In Kornbrot et al. (2007),

Wall and Harwin (2001) and the first experiment of Unger et al. (2010), the probe was modeled with an infinitely small tip, which, when in contact with the surface, produces a force proportional and opposite to the penetration depth into the virtual surface. The stimuli considered were sine waves of varying spatial period. The first two studies found that as spatial period increases, the roughness perception usually decreases in a linear fashion. Somewhat similarly, Unger et al. found the response exhibited a bipartite behavior, being relatively flat for periods less than 2 mm and with a decreasing log-log slope for larger periods. Perhaps more relevant to the present study, though, are their results from creating a trapezoidal grating texture with a virtual spherical probe, as it considers a probe of finite diameter to which Klatzky's drop point theory is applicable. For this implementation they found subjective roughness to be a sigmoidal logistic function of the texture period, increasing with spatial period. One important difference between their device and a single point matrix display is that with a single point matrix display the probe is real, contacting the finger, not virtual.

What previous results with both real and virtual textures mean for a matrix display is not easily discernable. It is essentially an array of probes which create patterns of spatial deformation on the fingerpad. However, the quasi-static patterns created, due to the finite spacing of the pins, are not the same patterns as for a real grating. This means that Taylor and Lederman's model cannot be implicated to predict the results. As stated above, changes in groove width of a virtual texture would instead be manifested as a change in the rate of pin activation as the device is scanned along the display surface. Vibratory cues are therefore present in this device, but there are multiple points of contact and frictional cues are absent.

Adaptation

Adaptation, the reduction in tactile sensitivity following a period of vibrotactile stimulation, has been found to occur within, but not across, the channels of the tactile sensory system (Gescheider, Wright, and Verrillo 2009). Because the four channels are primarily excited by different frequency ranges, a stimulus of a certain frequency can be used to reduce the sensitivity of a certain channel. In experimental work, selective adaptation of tactile sensory channels can be used to implicate those channels in the perception of certain stimuli. Work by Lederman et al. (1982) found that although adaptation to a 20 Hz stimulus (known to excite the FA I channel) and 250 Hz stimulus (known to excite the Pacinian or FA II channel) reduced the perceived magnitude of a test stimulus of 20 Hz and 250 Hz, respectively, no effect of adaptation at these frequencies was found on the perception of roughness of square-wave gratings with groove widths equal to or greater than 0.335 mm and ridge widths equal to or greater than 0.295 mm. Hollins, Bensmaia, and Washburn (2001) found that the discrimination of fine textures (2-D truncated pyramid arrays with spatial periods less than 100 μm) was impaired by vibrotactile adaptation of the Pacinian (FAII) channel (at adaptation frequencies of 100 and 250 Hz), but the discrimination of coarse textures (spatial period greater than 100 μm) was unaffected.

Hollins, Lorenz, and Harper (2006) examined adaptation to textures composed of 2-D arrays of truncated pyramids as opposed to vibrating stimuli. The spatial period of the textures varied from 124 up to 1416 μm, spanning the micro-texture / macro-texture divide. The adapting stimulus was also one of the test stimuli, a texture with a spatial period of 416 μm which was initially presented for a period of one minute prior to each block, and then presented for 20 seconds prior to each test stimulus. When the textures were explored with a handheld probe, adaptation caused the perceived roughness of the test stimuli to decrease as compared to a

control condition using a flat surface. When the textures were explored with the bare finger, however, adaptation was only observed for test stimuli with spatial periods less than 200 μm (the micro-textures). These results support the duplex theory of texture perception and also demonstrate the differences in perception between direct and indirect touch.

The latter study is important to this thesis for two reasons: 1) it demonstrates that adaptation of the tactile sensory system can occur after texture exploration, and 2) it demonstrates that texture adaptation can affect individual tactile sensory channels but not others, just as distinct vibratory stimuli can adapt specific tactile sensory channels. No study has yet examined the effect of texture adaptation when textures are explored through a haptic matrix display. For a system that can only present limited spatial cues as compared to direct touch, texture adaptation could pose a significant problem.

Outline of Thesis

In order to investigate the production and perception of virtual textures on a haptic matrix display device, some improvements were in order; the most important being the correction of the frequency mismatch between the commanded and actual frequencies. This was important to correct so that the results of experiments conducted with this device may be generalized to other matrix display systems. Section 3 presents these modifications. After these improvements, however, it was determined that a multi-level display would enhance the capability of the system to portray a much wider variety of textures, and so the device was redesigned to accommodate this added feature. The design of the multi-level haptic matrix display, including a discussion on the textures which can be created, is presented in Section 4. Section 5 presents the three main experiments which were conducted in this thesis. Experiment 1 was conducted to investigate how square-wave gratings, varying primarily in groove width, are perceived through a haptic matrix display and, consequently, to define design parameters for the construction of more complex textures. Experiment 2 examined the perception of square-wave gratings varying in ridge width, since ridge width was also found to be a significant factor in Experiment 1. Finally, Experiment 3 examined the effect of adaptation to a texture displayed on a matrix display, and compared it with texture adaptation when analogous physical textures were explored with a handheld probe and bare finger. The intention was to shed light on the possible problem of texture adaptation when a matrix display device is used, as well as to allow a comparison of texture perception through such a device to the more thoroughly studied probe and bare finger cases.

3. Preliminary Modifications

Although the new haptic matrix display device described in Section 2.3.1 improved upon the VT Player and Optacon, it still had some problems which affected its use; namely, (1) a small, but noticeable, time delay of 40 ms between movement of the device and pin actuation, and (2) error between the specified and actual frequencies of pin vibration. As stated in Section 2.3.1, cost was an important design consideration for this device, due to the intended user population. In order to remedy the frequency problem without the added costs of extra hardware, a new software driver was built which was capable of delivering discrete, yet accurate, frequencies. The software revisions also reduced the time delay, which had been attributed to a software lag (Owen et al., 2009). Thus, the device now quickly and accurately delivers an adequate number of frequencies despite the limitations of using a low-cost data acquisition system.

3.1 Correction of Frequency

It was noticed that the frequency at which the pins were actuated did not match the driving frequency which was specified. Although in many cases the error in frequency was small, in some cases the error was large. For applying any knowledge gained only to this device, frequency does not need to be precise as everything is relative; however, in order to generalize to other devices, the frequency needs to be well specified. For this reason, the software was redesigned with the purpose of correcting the error between the commanded and actual frequencies.

The first part of the new system that was sought was a reference for the program to ensure an accurate measurement of time. Often, commercially available data-acquisition

systems include a clock, typically on the order of 1 megahertz. However, with our design constraints such that it was imperative to minimize cost, the data acquisition system we used (National Instruments USB-6501 24-line Digital I/O) did not contain an on-board clock. We next looked to the host computer for a time reference. LabVIEW offers a 1 KHz clock which outputs the system time in units of milliseconds – it is a counter, the output of which changes every millisecond. Due to its ready availability and integration into the LabVIEW development environment, this was chosen as the time reference for the algorithm.

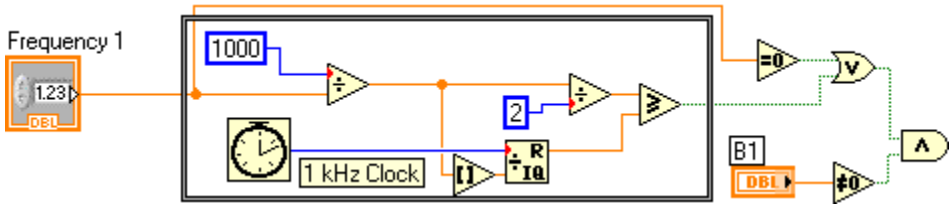

Figure 3. Enlarged view of frequency-generating algorithm.

Figure 3 above shows the frequency-generating algorithm for a single pin, based on the 1 kHz system clock. A given frequency (passed into the program from MATLAB) is divided into 1000. If, for example, the specified frequency is 10 Hz, 10 divided into 1000 yields 100. Assuming a 50% duty cycle is desired, this number is then divided by 2; for the present example, 100 divided by 2 yields 50.

At the same time, the quotient (100 in the present example) is rounded to the nearest integer and then divided into the system clock. Although the system clock counts to a very high value, what is sought from this division is the remainder from the operation, obtained by the modulus function in LabVIEW. To continue with our example, if at runtime the system clock reads 236376, the modulus of its division by 100 is 76.

After these calculations, the algorithm consists of logical operators. A comparator is now formed, measuring the input (the modulus from the system clock – in our example, 76) to the threshold (the specified percentage of quotient of the frequency divided into 1000 – in our example, 50). In order to send a high signal of the driving square wave, and thus to activate the pin, the modulus must be greater than the threshold. Since 76 is greater than 50, the output of this comparison in the present example is a logical TRUE.

In the case that frequency is specified to be zero, this is understood to command the pin to stay constantly up (if it is activated). For this reason, the frequency input is sampled and a logical operator determines if it is equal to zero. The logical output of this operator is fed, along with the result of the comparator just described, into an OR gate. Thus either condition (the modulus being above threshold, or frequency equal to zero) will output a binary TRUE. This output constitutes the primary driving waveform.

Finally, it is required that the pin be activated for the pin to rise at all, for any specified frequency. The pin state (either a 1 or a 0) is sent from MATLAB and is received as an input to the LabVIEW program along with the specified frequency. If this value is a 1, it passes (by means of a logical AND gate) the primary waveform through to the Data Acquisition Assistant module, which controls the interface to the NI USB-6501. Conversely, if the pin is not activated, the output of the AND gate will be a logical FALSE, and the pin will not be raised.

The block diagram of the modified LabVIEW driver is shown below in Figure 4. The box to the right receives input from the mouse buttons and was left unchanged from the previous version.

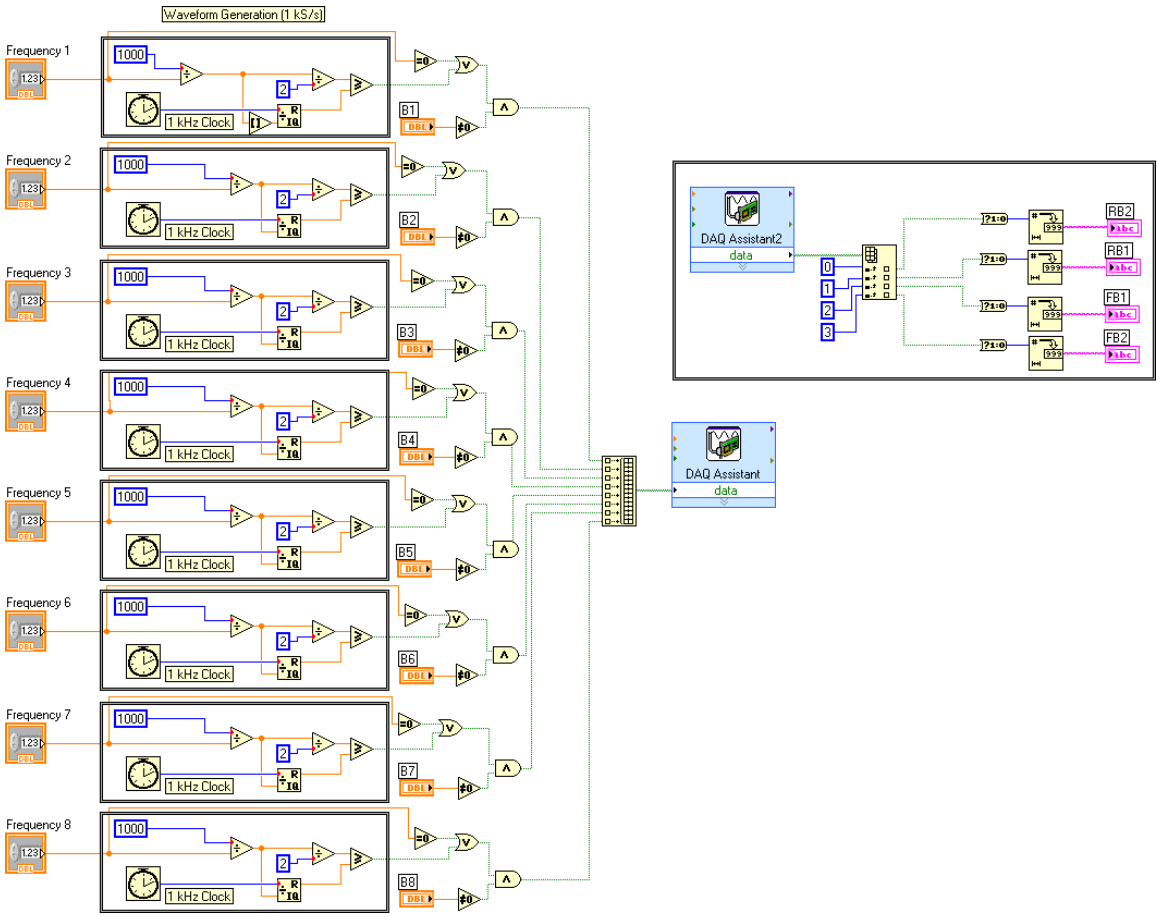

Figure 4. The updated LabVIEW driver.

3.2 Reduction of Delay

As a result of the new algorithm, the call from MATLAB to the compiled DLL took much less time than previously was the case; the entire loop was measured as running at 1 msec. This result was unintentional, but welcome.

3.3 Discussion

The use of the 1 KHz clock limits the frequencies that can be elicited by the system. This is due to the nature of the algorithm – division of frequency into 1000 yields quotients that are

increasingly close as the frequency increases; rounding those quotients to the nearest integer means that for a range of input frequencies, only one frequency will be elicited. This phenomenon is demonstrated below in Figure 5.

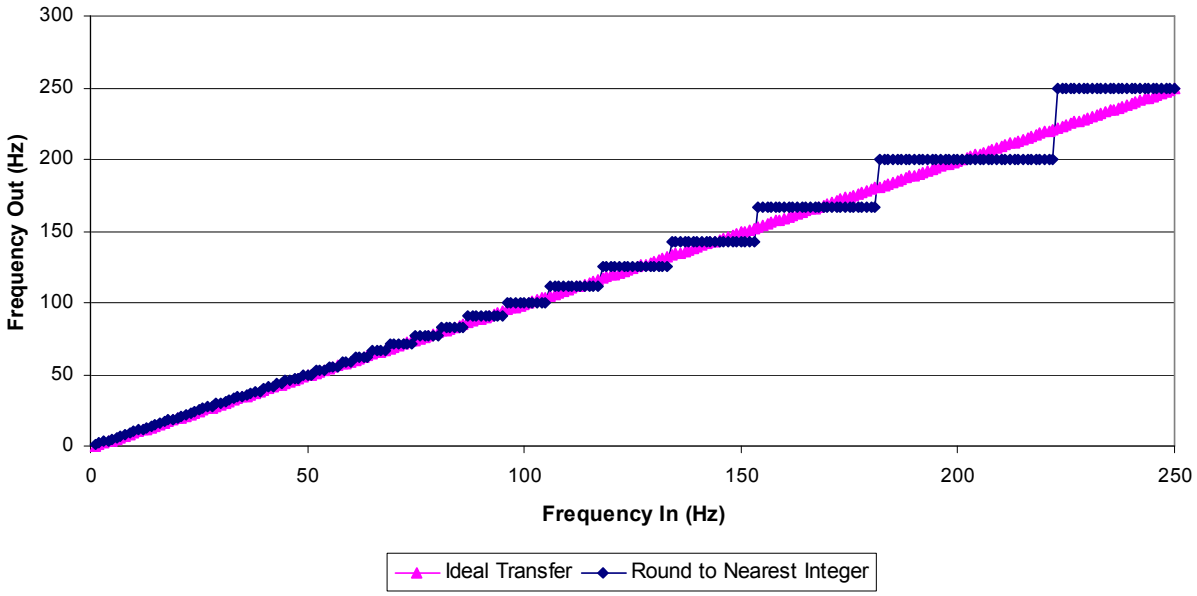

Figure 5. Frequency transfer for 1 kHz clock.

This outcome is acceptable for three reasons. Firstly, and most importantly, as our aim is to encode different parts of visual images and diagrams with distinct textures that can be tactually perceived as different, we do not require a continuous set of frequencies. Second is the fact that the frequencies of vibratory signals, as they increase, must be increasingly spaced apart in frequency in order to be perceived as distinct. Third, resonance was observed for the piezoelectric bimorphs constituting the actuators of the Braille cell at 180-190 Hz. This limits the desired frequency to 150 Hz at a maximum.

The frequency limitation imposed by the resonance does not only mean that square waves cannot be generated at that frequency; it also has implications for the production of textures and any experimental design. Because this is a dynamic system, the exploration of non-vibrating,

spatial square waves, or any type of spatial periodic pattern, will in turn produce a frequency equal to the product of the spatial frequency of the pattern and the exploration speed. In experimental work, the exploration speed should be kept below that which would, in conjunction with the highest spatial frequency, exceed 150 Hz.

4. Design of a Variable Amplitude Display

The modifications made to the tactile mouse described in Section 3 were completed in order to better achieve the goal of creating a tactile interface to provide non-visual access to computer graphics. While these improvements allowed the device to accurately display a moderately large set of frequencies, the amplitudes able to be displayed were limited to a binary on or off. Expanding the capabilities of the device in this dimension to display multiple amplitude levels would increase the number of combinations of dimensions (such as amplitude, frequency, and spatial arrangement) able to be displayed.

Van Erp (2002) has suggested that no more than four different amplitude levels be used to encode information. Based on this specification, it was decided to build a device which was capable of displaying four levels of amplitude. Van Erp has also suggested limiting frequencies to nine different levels. Although our device is capable of creating waveforms with many more frequencies, this combination of three non-zero amplitude levels and nine frequencies alone could generate twenty-seven different textures; varying the spatial layout of actuated pins based on location on the graphics tablet would yield a myriad of potential textures. Furthermore, a device capable of displaying multiple amplitudes could be used for such applications as a haptic drawing system for blind individuals in which the highest or lowest amplitude level was reserved for a reference grid, or for displaying text on graphics where Braille characters could use the highest amplitude level.

A low-cost solution was thus pursued to enable a 4-level amplitude display; the required changes to the device were sufficient in magnitude to constitute a new generation of the haptic matrix display device. This section chronicles its design and development.

4.1 Hardware Design

In order to keep the cost of the device low enough to be affordable to the intended user population, it was desirable to add as few new components to the previous iteration of the device as possible. Aiding this endeavor was the fact that many of the hardware components already in place did not directly affect the driving of the pins. Thus the mouse casing, oscillator circuit, and graphics tablet remained unchanged. Also kept were the 200V power supply and the Braille cell, as the inclusion of the commercially-available actuator and power supply kept design time and cost low. More importantly, however, the deflection of the piezoelectric bimorphs used to actuate the pins could be controlled as a function of the voltage applied to them. This actuator, by its nature of operation, was already ideal for a system designed to deliver multiple amplitudes of deflection – it only required multiple driving voltages to achieve the specification. Because the driving electronics of the previous generation of the device only took a single digital bit input per pin, and output either the full voltage or zero voltage, this portion of the device needed to be redesigned.

Since the data acquisition unit already utilized (National Instruments USB-6501) had sufficient unused digital output lines, a circuit which took a 2-bit digital signal as the input for each pin was conceived. This input could be fed into a 2:4 decoder which could signal four different voltages to be sent to the Braille cell.

Having settled on the decoders, a switching mechanism was required to select the various voltages to drive the piezoelectric bimorphs of the Braille cell. The original SPST relays used to switch the pins either on or off in the previous design were considered, but because four would be needed per pin and thus thirty-two per device, these relatively expensive components were not chosen. Next examined were discrete high-side power MOSFET switches, and a great solution

in the *Art of Electronics* was found, only to find that the required logic-to-high-voltage level translator chip had been discontinued and nothing similar seemed to be available. The high-side solution required a gate voltage near the high rail, which would be complicated to provide, and a low-side switch solution would not work. Due to these difficulties, the relay solution was reconsidered. It was noticed that the previous design used two relays, tied together, in order to provide a return to ground. Since ground is one of the desired voltages – the piezoelectric bimorphs actually rise maximally when driven to ground, with respect to a 200 V reference – only one photorelay needs to be connected to ground. By using a DPST relay that is either all form A or form B (normally open or normally closed), just two relay DIP chips per pin would be sufficient to control the four voltage levels desired. Furthermore, high-voltage Toshiba photorelays were sourced which were less expensive than the ones previously used.

The required voltages were obtained by incorporating three voltage dividers to step down the highest voltage to two intermediate voltages and then to ground. Resistors values of 10 kΩ were found to work well, providing sufficient current to the device while remaining relatively large enough to retain the voltage level at DC. The voltage divider resistors were made to be potentiometers so that the voltage levels, and thus the amplitude levels, could be adjusted. An initial test of the variation of these potentiometer values found that resistances of 20 kΩ, 5 kΩ, and 5 kΩ, providing voltage levels to the Braille cell of approximately 170 V, 60 V, and 30 V, respectively, yielded the most distinct individual levels of amplitude. These approximately logarithmically decreasing voltage values correspond to an approximately logarithmic change in amplitudes, which would be expected to be perceived as linear changes in magnitude. Although the equipment required to accurately measure the changes in amplitude was not available, pilot

testing (presented in Section 4.5 below) revealed that these levels were indeed distinct from each other.

The device, however, is not run at DC. When the input frequency was increased, the voltage supplied to the Braille cell at the output of the circuit quickly declined. This is shown below in Figure 6.

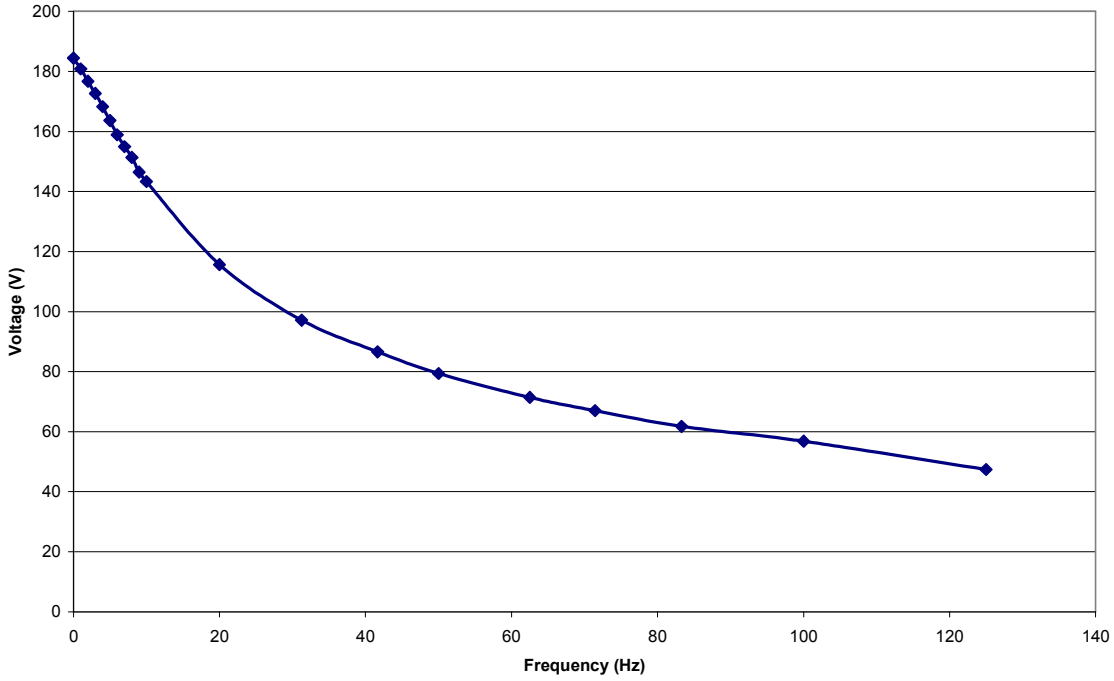

Figure 6. RMS voltage of Metec-AG power supply as a function of frequency.

After much searching, it was determined that the decoders were giving multiple activation signals during the transition period between two pin levels – the incidence of which greatly increased as the driving frequency increased. The enable pins of the decoders had been wired to ground, so that they were always enabled, but clearly this posed a problem. It was resolved to control each pin with a 3-bit digital signal: two bits to select the driving voltages, and one bit to selectively enable the decoder. This solution disabled the encoder for a very brief

amount of time in response to changing commanded amplitude values, and effectively fixed the problem. The final circuit for a single pin is shown below.

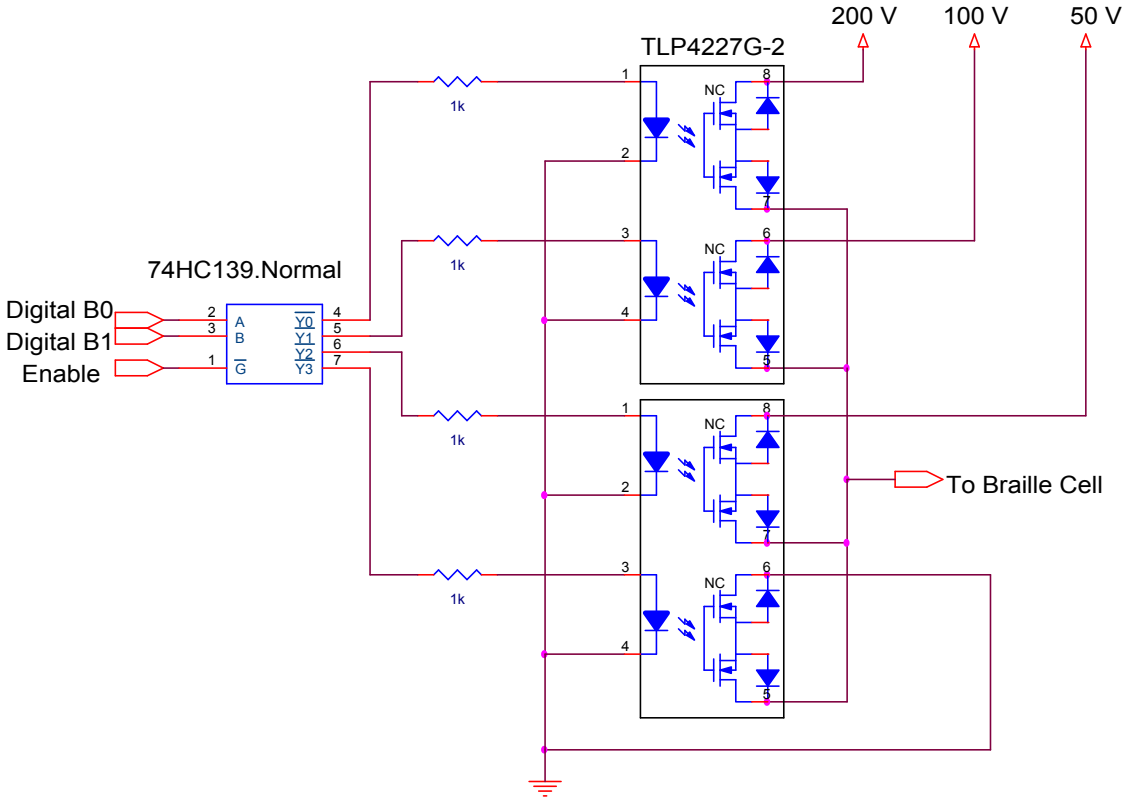

Figure 7. Circuit schematic of driving electronics for a single pin.

4.2 Software Design

The software to control the new driving electronics was easily adapted from the modified software previously described in Section 3. Instead of taking a 0 or 1 control signal from MATLAB to turn each pin on or off, the LabVIEW program now accepts a 0, 1, 2, or 3 to specify the desired voltage level. A case-structure architecture was employed, with each case to be selected by the voltage control number from MATLAB. All cases with the exception of the 0 case incorporated the frequency-generating algorithm previously described. The cases are shown

below in Figures 8-11. For the 0 case, two Boolean FALSE signals were wired to the two output terminals serving as the 2-bit voltage control output. For the 1 and 2 cases, the output of the frequency-generating algorithm was tied to one of the output terminals, while a FALSE signal was connected to the other terminal. The orders were switched for cases 1 and 2 to

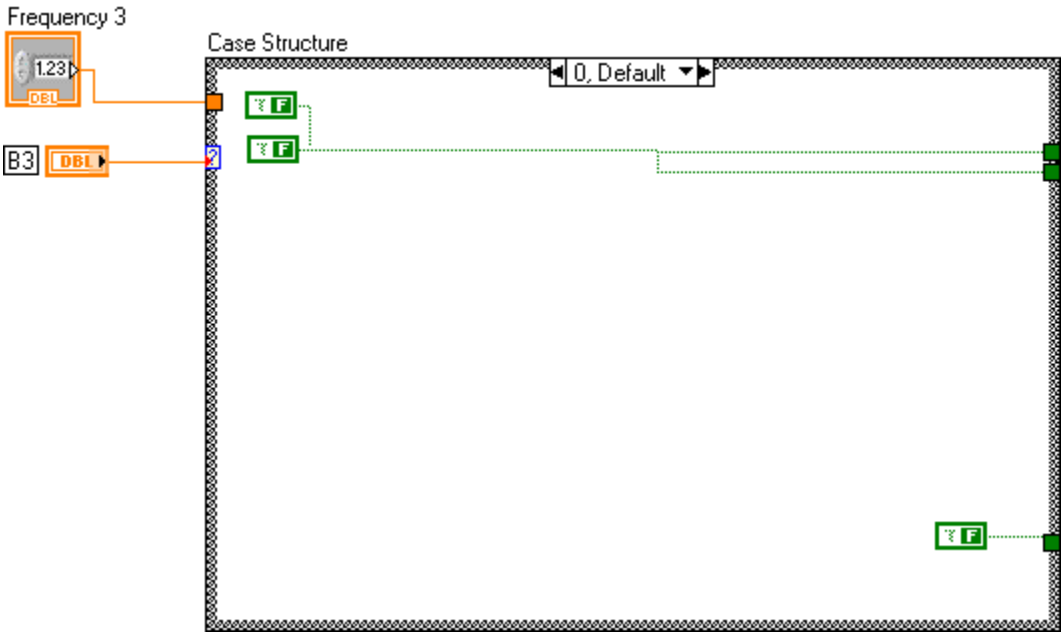

Figure 8. Enlarged view, case of Amplitude Level = 0.

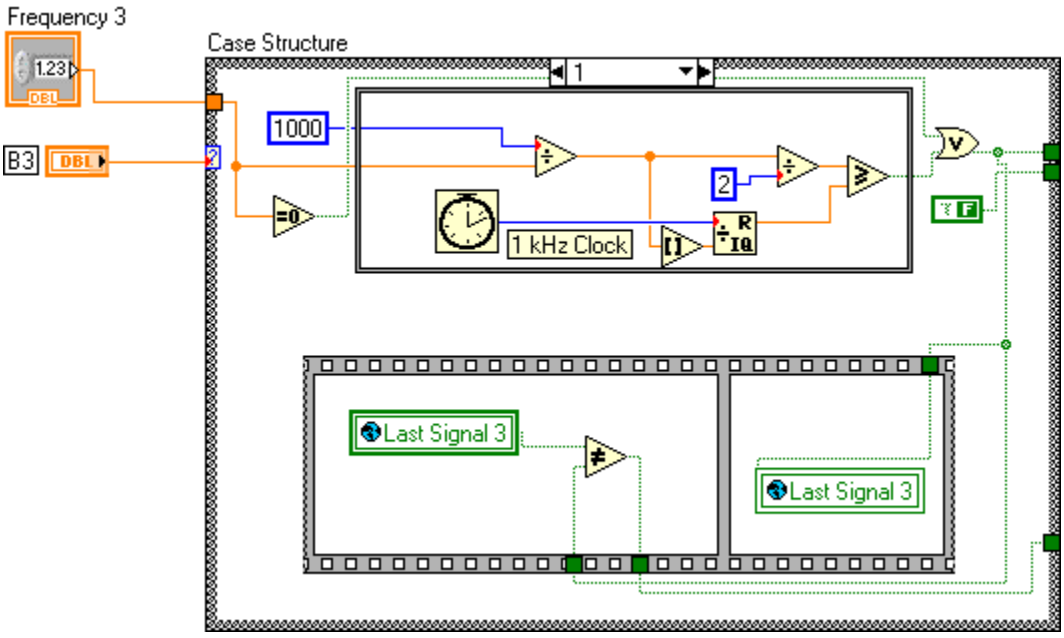

Figure 9. Enlarged view, case of Amplitude Level = 1.

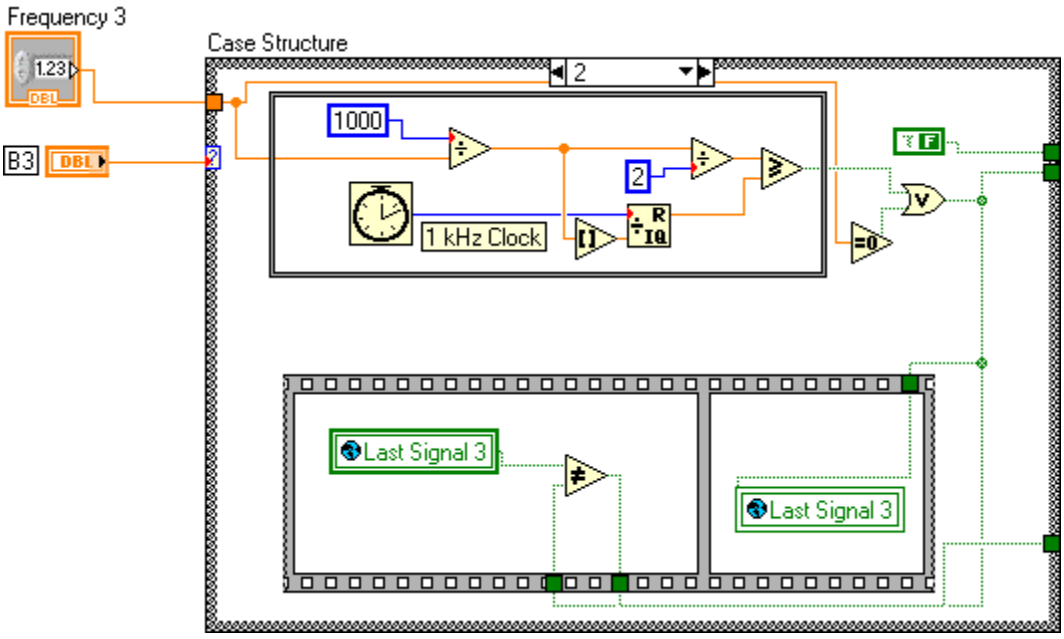

Figure 10. Enlarged view, case of Amplitude Level = 2.

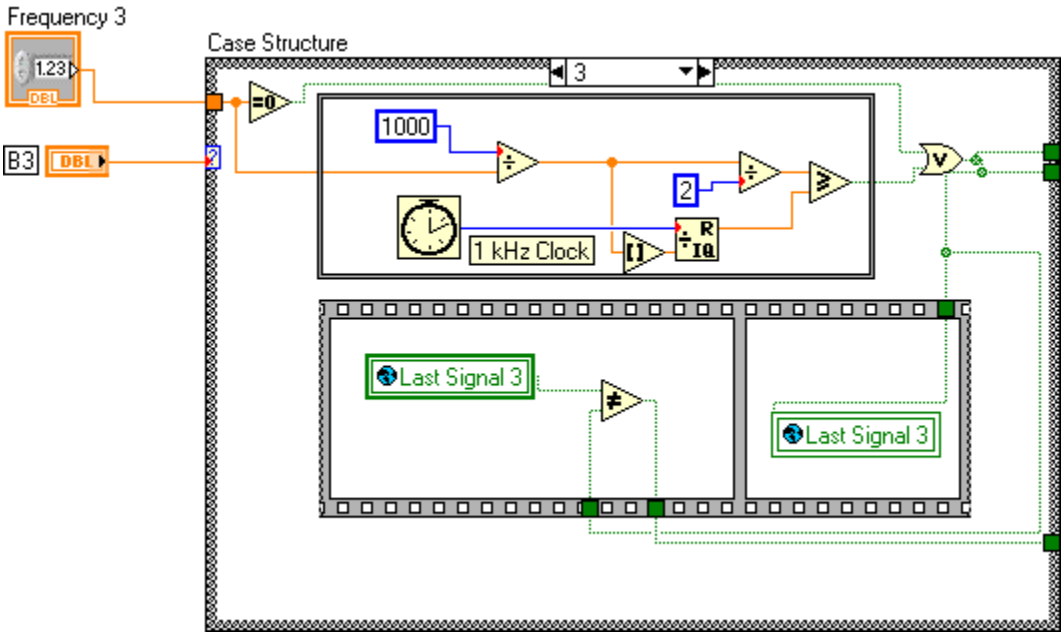

Figure 11. Enlarged view, case of Amplitude Level = 3.

correspond to the binary representations of 1 and 2. In this way, a square-wave signal would cause the 2-bit voltage control signal to oscillate between binary 1 or 2 and 0. For the case 3, the output of the frequency-generating algorithm was connected to both output terminals, to provide either a [1 1] or a [0 0] signal.

When the decoder problem was found, a third control bit needed to be added for each case to control the enable pin of each decoder channel. It was desired that the decoder be enabled at all times except during the transition between voltage levels, corresponding to the decoder switching. To achieve this, a global variable was saved which stored each pin's output. A structure was put in place to compare the previous output to the current output; if the two were different, the enable signal would go FALSE. If the two outputs were the same, that would indicate that the voltage level was not changing and thus the decoder would still be enabled. A timed structure was used to ensure that the comparison took place before the new output level

was saved. These structures can be seen in Figures 10-13, with the exception of the 0 case. Note that this feature would only be utilized by pin channels driven at a frequency and amplitude greater than zero.

The 3-bit outputs from all eight pin channels were assembled and fed into the DAQ Assistant module, which communicated these signals to the NI USB-6501 digital I/O board. The complete LabVIEW program, containing the eight individual voltage-control case structures and their connections to the output; is shown below in Figure 12.

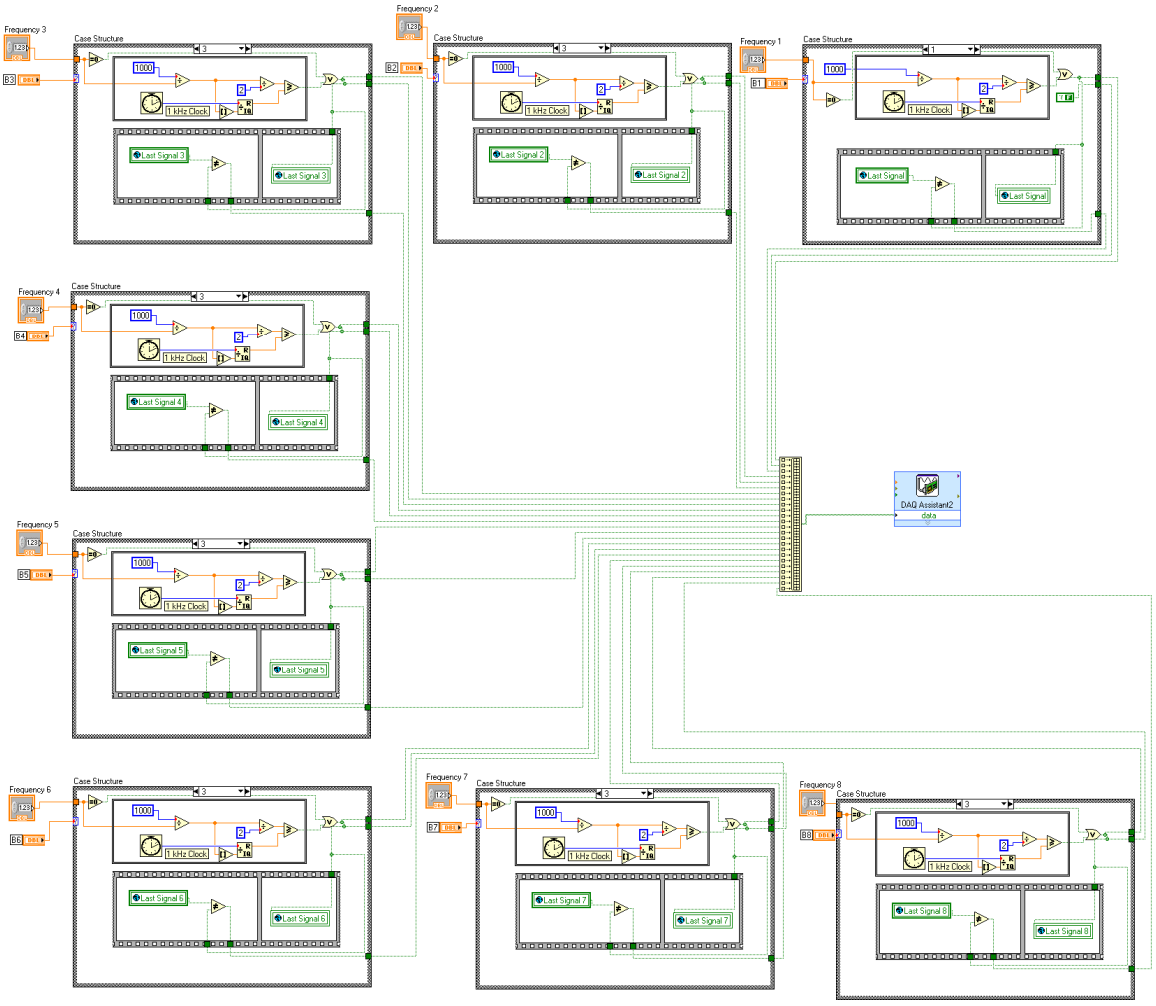

Figure 12. The new LabVIEW driver.

4.3 Texture Design

This version of the haptic display device system, as with the previous version, was designed to be run from MATLAB. In order to translate visual images and diagrams to a tangible format displayed with this system, some way of mapping amplitude levels and frequencies to specific pixel locations was required. A texture map was conceived which would include an amplitude level (0, 1, 2, or 3) and a frequency for every pixel on the computer screen, contained within a three-dimensional matrix with the number of rows equal to the screen height in pixels, the number of columns equal to the screen width in pixels, and a depth of two (two elements for every x-y location; an amplitude level and a frequency). These texture maps could be created labor-intensively by manually changing every element to the desired amplitude and frequency; alternatively, numerical algorithms could be used. The textures that were subsequently used in the experiments discussed later in this work were generated by numerical algorithms.

4.4 System Overview

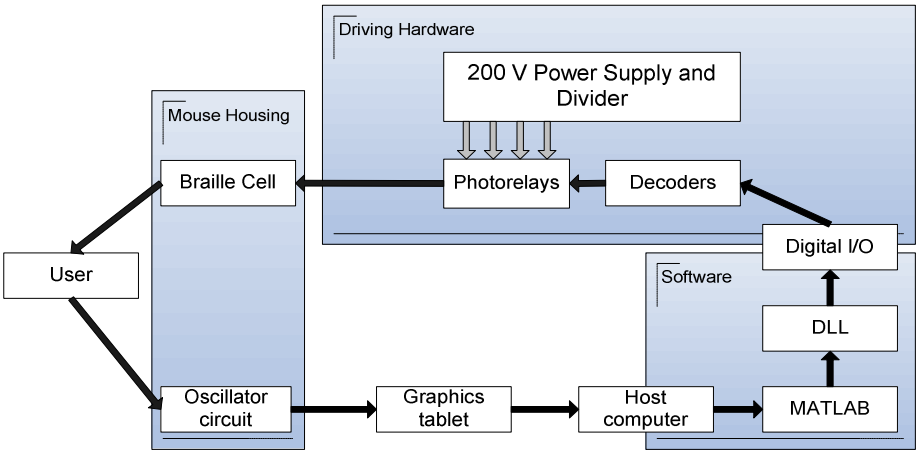

Figure 13. Haptic mouse block diagram.

The block diagram above shows the components of the haptic matrix display. The system works by first selecting a texture map. As the user moves the mouse, which houses the oscillator

circuit, the position of the mouse on the graphics tablet is communicated to the operating system and found by the MATLAB program. The program then searches for the elements of the texture map which correspond to the pixel position of the cursor, and passes the corresponding amplitudes and frequencies of all eight pins to the compiled LabVIEW DLL. This driver produces digital waveforms which are output through the digital I/O to the inputs of the decoders. The appropriate voltage level channel is then selected and the appropriate photorelays close to allow current to pass to the Braille cell piezoelectric bimorphs. The bimorphs deflect, raising the pins of the Braille cell.

4.5 Discrimination and Identification of Amplitudes

Upon the successful design and construction of the system described in above, some preliminary experiments were completed to assess the usefulness of the new features. Because the maximum displacement of the pins of the Braille cell is relatively small (0.45 mm), it was desired to know whether intermediate amplitude levels could in fact be discriminated from each other and the maximum amplitude level. Also, as these amplitude levels would be used in the creation of textures subsequently used to display different objects and object parts in virtual tactile diagrams, we wanted to know if the different amplitude levels could be identified as well.

Five sighted subjects from the lab participated in an informal experiment in which they were simultaneously presented with two random amplitudes from the four levels (0, 1, 2, or 3) and asked whether the two amplitudes were the same or different. The amplitudes were presented with static (0 Hz) raised pins, the pins vibrating at 30 Hz, and the pins vibrating a 100 Hz. Each subject was blindfolded and wore headphones playing a soft pink noise in order to mask any device sounds. The amplitude levels were presented on the matrix display device according to the position of the device on the graphics tablet; one amplitude was presented on the

left side, and the other on the right side. There were 16 combinations of amplitudes, presented in one of two positions (left or right) and at 3 different frequencies. These were randomly presented in four blocks (with a total of 48 trials per block). The two amplitudes were always displayed at the same frequency. The first block was treated as a training block and its data was not analyzed.

All amplitudes levels were found to be able to be discriminated from each other 96% of the time, and identified greater than 84% of the time. The results are shown below in Figures 14 and 15.

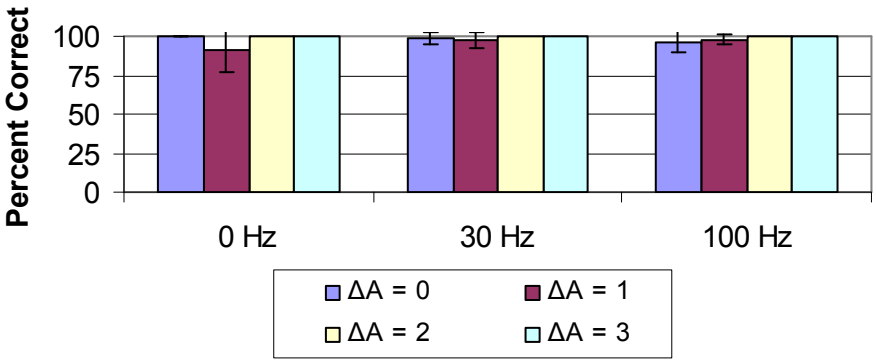

Figure 14. Average percent correct discrimination of amplitudes at a given frequency.

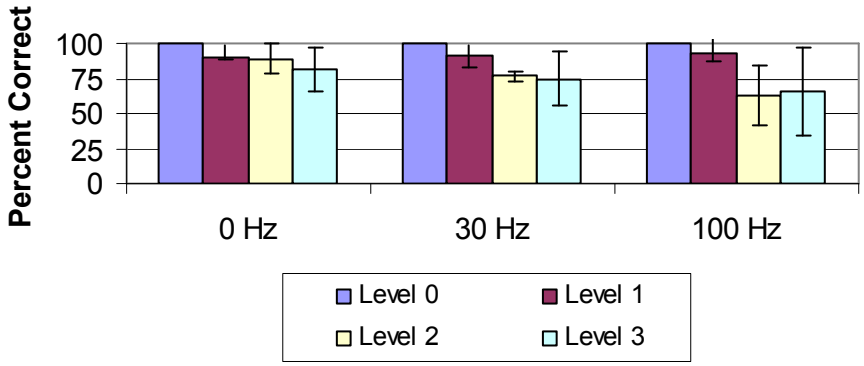

Figure 15. Average percent correct identification of amplitudes at a given frequency.

4.6 Discrimination of Multi-level Textures from Binary Textures

One of the most useful foreseen uses of providing multiple amplitude levels was the ability to create more complex and distinct textures. A very simple and preliminary investigation was devised to test whether textures composed of four amplitude levels felt distinct from those composed of two levels. Four sighted subjects from the lab participated in an informal experiment in which they were simultaneously presented with two textures of similar spatial layout. Four pairs of textures were used; within each pair each texture was composed of either four or two amplitude levels. The two-level textures of these pairs consisted of an array of circles, an array of squares, a square wave grating of large spatial period, and a square wave grating of small spatial period. The matching four-level textures consisted of an array of dithered cones, a truncated pyramid array, and two superimposed square wave gratings of large and small base periods. These two last gratings were essentially square waves of square waves, with the high side oscillating between levels 2 and 3 and the low side oscillating between levels 0 and 1. The pairs are shown in Figure 16 below.

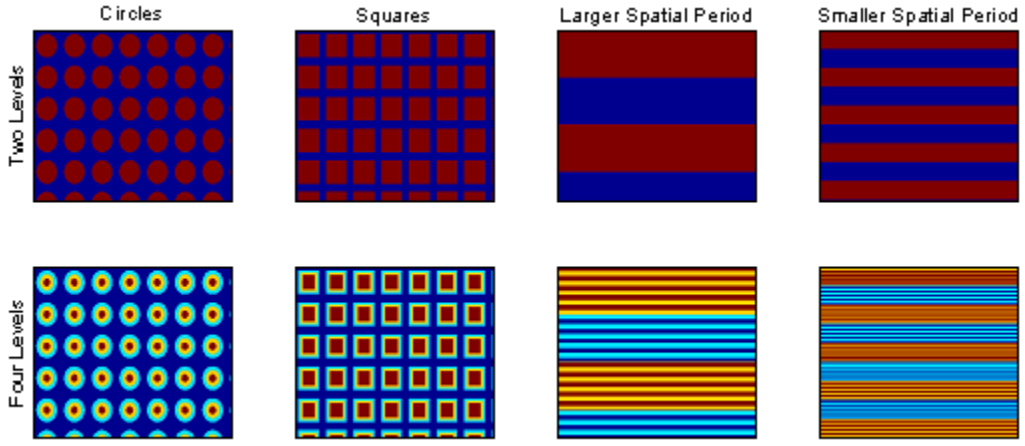

Figure 16. Two- and four-level texture pairs.

Each subject was blindfolded and wore headphones playing a soft pink noise in order to mask any device sounds. The textures were presented on the matrix display device according to the position of the device on the graphics tablet; one texture was presented on the left side, and the other on the right side. Sixteen pairs were randomly presented in each of four blocks, consisting of all eight combinations of textures, including variations on the positions (left or right) of each texture. Each subject was asked whether the two textures were the same or different. The first block was treated as a training block and its data was not analyzed. Textures composed of four amplitude levels were found to be able to be discriminated from textures composed of only two amplitude levels over 79% of the time on average. The results for the individual texture pairs are shown below in Figure 17.

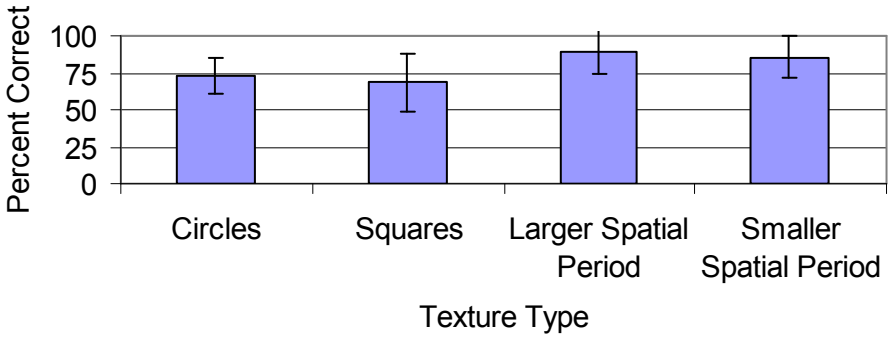

Figure 17. Average percent correct discrimination between binary and multiple amplitude levels.

While this experiment only tested eight different textures, there exists a myriad of possible textures that could be created. However, it was determined that more basic information regarding the perception of textures though a matrix display such as this one was needed before any further texture design,. The experiments presented in Section 5 fulfill these aims by understanding how the perception of texture, in particular roughness, with our matrix display

compared to what is known about other types of texture perception (i.e., using a bare finger or either a physical or virtual probe). They constitute the main experimental work of this thesis.

4.7 Drawing Program for Visually Impaired Persons

As stated above, a system capable of displaying multiple amplitude levels could be used to create a computer drawing program for people who are blind or visually impaired. Such a drawing program was conceived, consisting of an easy-to-use multimodal user interface that would not only allow blind and visually impaired persons to create and feel drawings on a computer, but also be useful to sighted people wishing to create texture-encoded images. More information on this concept can be found in (Headley and Pawluk, 2010b).

4.8 Conclusion

A low-cost, multiple amplitude haptic matrix display has been built, along with driving software, with the capability of displaying four different amplitude levels, according to the specification of van Erp (2002). Initial pilot work has shown an excellent ability of subjects to discriminate all four amplitude levels, but the highest levels are not always identifiable. The ability to correctly identify amplitude may drop off at higher frequencies. Another pilot experiment using a very small sample of pairs of two- and four-level textures showed an ability to distinguish textures composed of the different levels that was better for square wave gratings. These results are applicable to the design of textures, but are very preliminary; much more work is needed. This low-cost device will still be financially accessible to the intended user population of blind and visually impaired people, many of whom live below the poverty line, and may find additional applications such as a computer drawing system for visually impaired individuals.

5. The Perception of Vertical Gratings through the Haptic Matrix Display Device

This section presents the three main experiments which were conducted in this thesis. Experiment 1 was conducted in order to investigate how square-wave gratings, varying primarily in groove width, are perceived through a haptic matrix display and, consequently, to define design parameters for the construction of more complex textures. Because ridge width was also found to be a significant factor in Experiment 1, Experiment 2 examined the perception of square-wave gratings varying in ridge width. Experiment 3 was motivated by the concern that adaptation to texture may have a negative effect when using texture encoded information on tactile diagrams. Experiment 3 examined the effect of adaptation to a texture displayed on a matrix display, and compared it with texture adaptation experienced when exploring textures with a handheld probe and bare finger, as we know that individuals can successfully use texture in tactile diagrams with the bare finger. Additionally, the experiment allowed a comparison of texture perception through such a device with texture perception through the more thoroughly studied probe and bare finger.

5.1 Variables Considered

The haptic display device we have created allows for the manipulation of the number of pins of the Braille cell activated and the height to which they are each raised. In conjunction with the driving software, the physical parameters of virtual textures can also be manipulated; for gratings, groove width and ridge width can be controlled. Groove width and ridge width are illustrated below in Figure 18. Changing these parameters can in turn change other dependent parameters, such as spatial period and duty cycle. All of these parameters are factors which may

influence the perceived magnitude of the roughness of a virtual texture. Experiment 1 examined the effects of groove width, ridge width, and the number of pins activated. The commanded height of the activated pins was kept to the maximum in order to keep the experiment to a reasonable length. Spatial period and duty cycle were not controlled as these parameters could be calculated from the groove and ridge widths for later analysis.

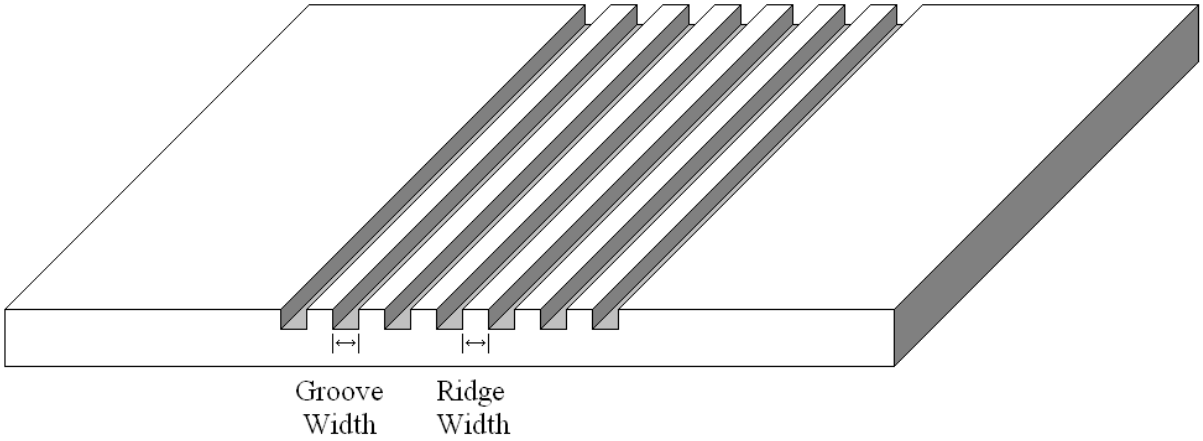

Figure 18. Stimulus grating with groove width and ridge width indicated.

Two additional parameters, contact force and exploration speed, may also influence the perception of roughness. With respect to contact force, this device is designed to be an open-loop system in order to keep cost to a minimum. Furthermore, the stiffness of the piezoelectric bimorphs of the Braille cell is unknown, and so the accurate measurement of contact force is difficult to procure. Thus the effect of contact force was ignored in this experiment. Before these experiments could proceed, however, additional pilot work was required to determine the effect of exploration speed on texture perception.

5.2 Effects of Speed on Texture Perception

For different modes of exploration of textures, speed has been found to have a varying effect on the perception of roughness. Lederman (1974) found that for exploration of coarse textures with

a bare finger, there was no effect of velocity on perceived roughness. However, when considering a probe, (Klatzky 1999) found that roughness estimates were affected by the speed with which the probe was moved (albeit with raised dot stimuli rather than square wave gratings). The latter has important implications for misconstruing textures when used in a real world situation (such as using texture on a map with a key). In order to determine if exploration speed affect the use of our display device, a pilot experiment was conducted.

Four sighted subjects from our laboratory explored four blocks of 32 virtual vertical gratings with the haptic display device. The dimensions of the vertical gratings varied by groove width (approximately 0.5 mm, 1 mm, 1.5 mm, 2 mm, 2.5 mm, 3 mm, 3.5 mm, 4 mm, 4.5 mm, 5.5 mm, 6.5 mm, 7.5 mm, 8.5 mm, 9.5 mm, 10.5 mm, 11.5 mm) and ridge width (0.5 mm and 3.5 mm), with both dimensions completely crossed. The textures filled the central display area of the graphics tablet used (Adesso CyberTablet 12000, 226 mm by 302 mm). Two blocks were explored with one of two speed ranges: 20 ± 5 mm/s and 40 ± 5 mm/s (the other two blocks used the other speed). Both the blocks were presented in random order, and the virtual gratings were presented in random order within blocks. An addition pilot with three sighted subjects repeated the experiment with only one active pin in the display.

The experimental procedure was based on the protocol used by Lawrence et al. (2007). Before the experiment began, each participant was trained to use a lateral back and forth exploratory procedure across the texture which spanned both the texture surface (horizontal distance) and a smooth surface (all pins retracted) at the horizontal edges (horizontal distances). The speed was calculated in the software and monitored by the experimenter; if the exploration speed was out of range, the subject was told to either slow down or speed up. On each trial, subjects explored the display area with the distributed haptic device and judged the roughness of

the virtual grating using the absolute magnitude estimation method (Zwislocki and Goodman 1980), in which he or she provided a positive, non-zero integer, decimal, or fraction representing the magnitude of the perceived roughness. The subjects were told that the number should be proportional to the roughness they experienced; if one texture was perceived as twice as rough another, its assigned number should be about twice as large. The results are shown below in Figures 19 and 20.

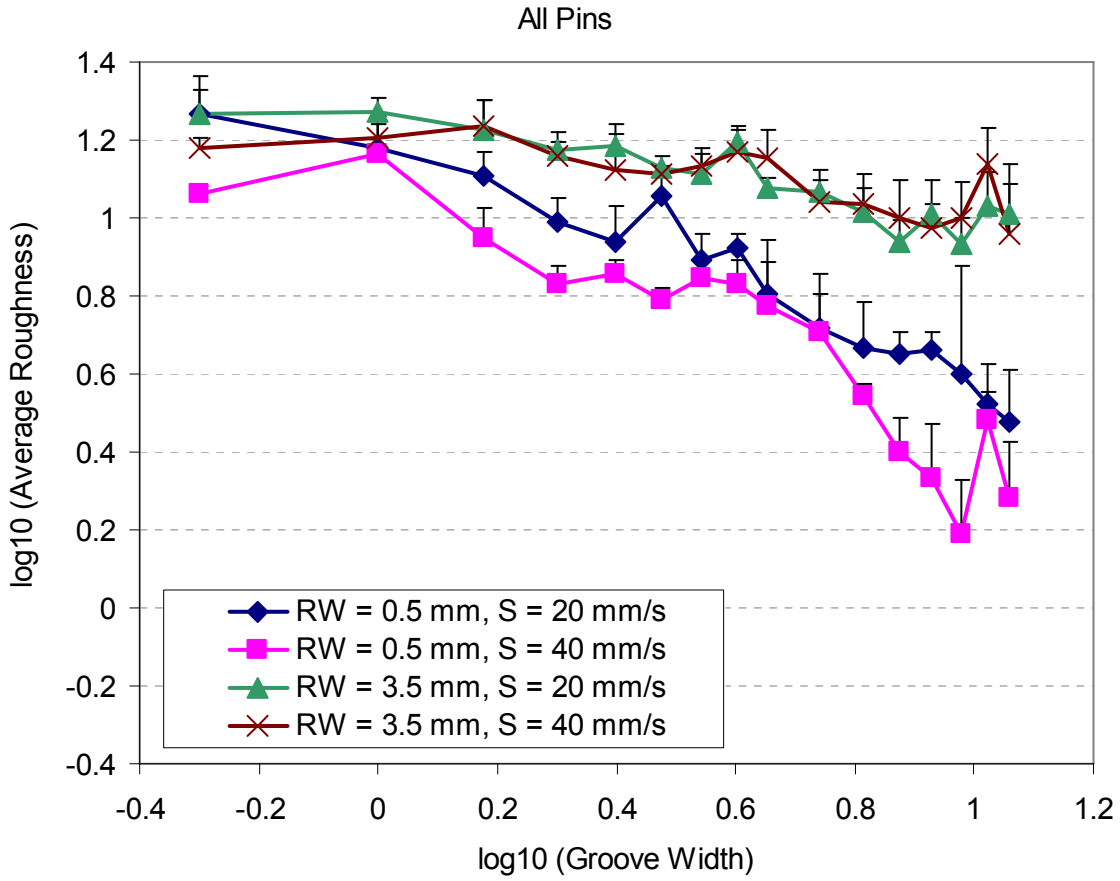

Figure 19. Results for pilot experiment examining effect of exploration speed on perceived roughness with all pins activated. RW = ridge width; S = speed. Error bars represent 1 SEM.

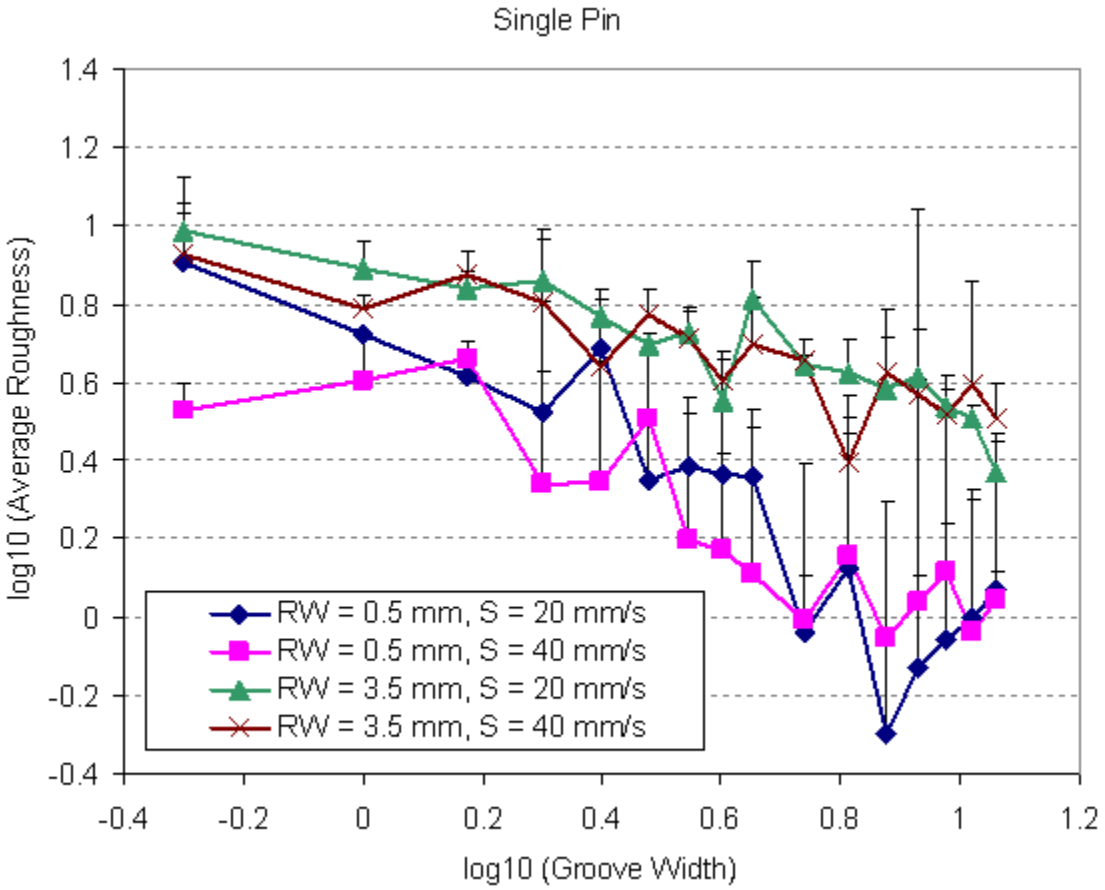

Figure 20. Results for pilot experiment examining effect of exploration speed on perceived roughness with one pin activated. RW = ridge width; S = speed Error bars represent 1 SEM.

Although the number of subjects in either experiment is too small for any significant statistical analysis, no striking difference was observed between the two speeds in either case. The speed was limited in this pilot experiment and in Experiment 1 to below 50 mm/s because of hardware limitations. The usable bandwidth of the system is 125 Hz (for generating vibrations); the total bandwidth is approximately 500 Hz, but the piezoelectric bimorphs exhibit resonance at around 185 Hz. The smallest ridge and groove width used in these experiments is 0.5 mm. Multiplying the bandwidth by this smallest ridge width yields the maximum exploration speed which can be used without missing the ridge; with the bandwidth of 125 Hz, this yields an exploration speed of

62.5 mm/s. Setting the maximum speed to 50 mm/s imparts a safe distance to the actual limit. Although speed effects may exist at higher speeds, because the use of this device is ultimately aimed at conveying information contained in graphics, a slow exploration speed in actual use is expected. Consequently, this is the speed range in which we are most interested.

In designing the experiment, two additional considerations were made. The first is whether the stimuli should be allowed to be actively or passively touched. Previous studies have found no difference between active and passive exploration (Lederman 1981); however, because the pins of the haptic display device do not move tangentially with respect to the finger, we believe active exploration to be an essential component in the construct of a mental model of texture for this particular device. For this reason active exploration was chosen over passive exploration. The second consideration is the population from which test participants should be recruited. Various studies examining the performance of blind subjects as compared to that of sighted subjects in tactile orientation and texture discrimination tasks have found differing results (Alary et al., 2009). Because this device (and other tactile matrix display devices) may find applications beyond the blind community, both blind and sighted subjects were enrolled and grouped separately

5.3 Experiment 1 – Groove Width

5.3.1 Methods

Participants

Seventeen subjects (ten females, seven males; mean age = 30.7 years, SD = 14.3 years) participated in the experiment. Of the seventeen, two subjects were totally blind and five subjects were visually impaired. All but three subjects reported being right-handed (one indicated she was ambidextrous, but completed the experiment using her right hand only). Participants were divided into two groups: those who were sighted (10) and those who were visually impaired (7).

Apparatus and Stimuli

The multi-level haptic matrix display presented in Section 4 was used to display the stimuli to each subject. During the experiment the number of pins that were activated was manipulated: either a single pin portrayed the texture with the others fully retracted, or all 8 pins portrayed the texture. A set of 32 virtual vertical gratings were used as texture maps. The dimensions of the vertical gratings varied by groove width (approximately 0.5 mm, 1 mm, 1.5 mm, 2 mm, 2.5 mm, 3 mm, 3.5 mm, 4 mm, 4.5 mm, 5.5 mm, 6.5 mm, 7.5 mm, 8.5 mm, 9.5 mm, 10.5 mm, 11.5 mm) and ridge width (0.5 mm and 3.5 mm), with both dimensions completely crossed. The textures filled the central display area of the graphics tablet used (Adesso CyberTablet 12000, 226 mm by 302 mm).

Experimental Design

Three completely crossed within-participant factors were included: Groove width (16 levels), Ridge width (2 levels) and Number of pins activated (2 levels). One between-participant factor was also included: Degree of visual impairment (2 levels). Each unique stimulus (grating and ridge width combination) was presented once for 32 trials per block. The blocks were assigned one of the two levels of number of pins so that the level of the second block differed from the level of the first block and that each level had two blocks per experiment. Four blocks were performed with a total of 128 trials.

Procedure

As with the speed pilot experiment, the experimental procedure was based on the protocol used by Lawrence et al. (2007). Before the experiment began, each participant was trained to use a lateral back and forth exploratory procedure across the texture which spanned both the texture surface (horizontal distance) and a smooth surface (all pins retracted) at the horizontal edges (horizontal distances). The participant was told the exploration speed would be limited to below 50 mm/s, and that their speed would be monitored throughout the experiment. If they exceeded 50 mm/s, they would be told to slow down.

On each trial, subjects explored the display area with the distributed haptic device and judged the roughness of the virtual grating using the absolute magnitude estimation method as with the pilot study describe previously in Section 5.2. Lines of varying length were presented either visually or haptically to the subject, who was asked to judge the magnitude of each line. A short line was presented first, followed by one twice the length. It was emphasized to the subject that the second assigned number should be twice as large as the first; in almost all cases, the subject appropriately assigned the number. A third line was presented which was much longer

that either of the previous two, in order to demonstrate that subjects should not limit themselves from a traditional 1-10 scale. Likewise a very short line was presented to emphasize that ratings can be less than 1.

5.3.2 Results

The logarithmically transformed average perceived roughness is plotted as a function of the log of groove width for both ridge widths and pin conditions used in the experiment in Figure 21. In general, for all conditions, as groove width increased, the average perceived roughness decreased.

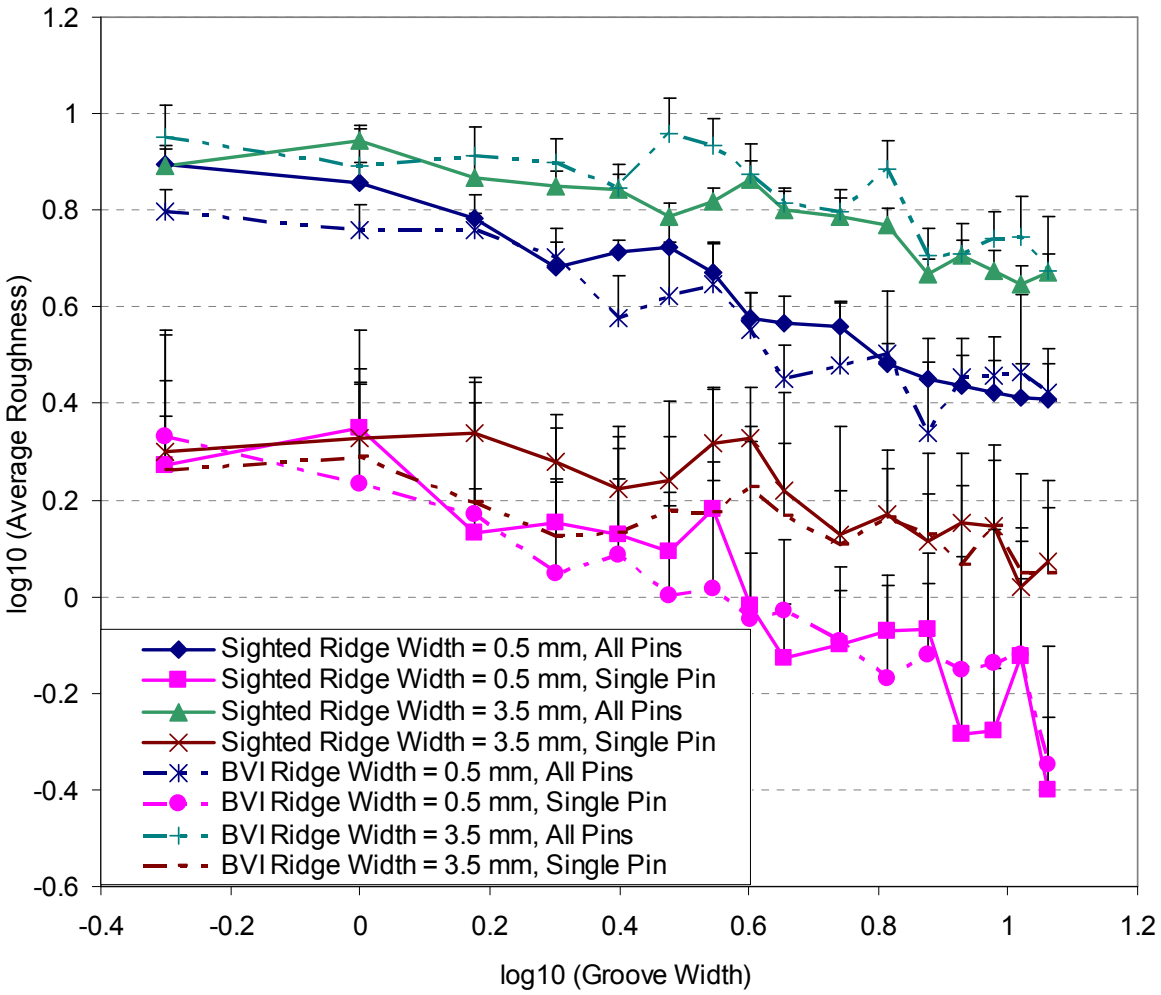

Figure 21. Experiment 1 results. Error bars indicate 1 SEM.

Linear approximations were fit to each of the four obtained psychophysical functions (relating them to a power law); these fits are shown in Figure A1 in Appendix A. The R^2 values for these fits are provided in Table 1, along with the R^2 values for quadratic fits. For the curves obtained with ridge width = 3.5 mm, a quadratic line proved a better fit (see Figure A2). For ridge width equal to 0.5 mm, however, a quadratic fit yielded only a small improvement in R^2

Table 1. R^2 values for curve fits for the results of Experiment 1.

Ridge Width	Number of Pins	Linear Fit R^2	Quadratic Fit R^2
0.5 mm	8	0.9449	0.9558
0.5 mm	1	0.8785	0.9045
3.5 mm	8	0.7818	0.9049
3.5 mm	1	0.6916	0.7872

Although the data for some individuals were noisy, all individuals generated curves similar in shape to the group means presented in Figure 21 (with the exception of one quadratic curve for one sighted individual when ridge width was held constant at 3.5 mm and only one pin was activated). The group means, then, represents what is truly happening in the individual cases and is not an artificial shape (see Kornbrot et al. (2007) for context).

Table 2. Significant ANOVA results for Experiment 1.

Effect	F	Significance	η^2
Groove width	41.198	<.0001	0.733
Ridge width	20.196	<.0001	0.574
Number of pins	85.452	<.0001	0.851
Repetition	15.405	<.0001	0.507
Groove width * Ridge width	37.918	<.0001	0.717
Groove width * Number of pins	30.088	<.0001	0.667
Groove width * Ridge width * Number of pins	41.246	<.0001	0.733

An ANOVA revealed significant main effects of groove width ($F = 41.198$, $p<.0001$, $\eta^2 = 0.733$), ridge width ($F = 20.196$, $p<.0001$, $\eta^2 = 0.574$), number of pins ($F = 85.452$, $p<.0001$, $\eta^2 = 0.851$), and repetition ($F = 15.405$, $p<.0001$, $\eta^2 = 0.507$) on the roughness perceived. Note that all four of these factors exhibited large effect sizes. Vision or lack thereof was not found to be a significant factor. The interaction of groove width and ridge width was found to be significant ($F = 37.918$, $p<.0001$, $\eta^2 = 0.717$), reflecting the observation that the rate of change of roughness as groove width increases was higher for the smaller ridge width of 0.5 mm (compare the slopes of the linear approximations for both ridge widths). The interaction of groove width and number of pins was also found to be significant ($F = 30.088$, $p<.0001$, $\eta^2 = 0.667$). The three-way interaction of groove width, ridge width, and number of pins was found to be significant ($F = 41.246$, $p<.0001$, $\eta^2 = 0.733$), reflecting the increased divergence between the rates of change in roughness as groove width is increased for the two ridge widths as the number of pins drops from 8 to 1.

5.3.3 Discussion

Although the mechanics of interaction between a matrix display and the fingerpad is very different than using the bare finger, a probe or a virtual probe, we will first compare our results to this previous data. Perhaps the closest in form to our response is that for virtual sinusoidal gratings using a force feedback point contact device, where the contact is modeled as an infinitely small point (Kornbrot et al., 2007, Wall and Harwin 2001, Unger et al., 2010). All these groups found that perceived roughness decreased linearly with increasing groove width, although Unger et al. (2010) found the slope to be flat for periods less than 2 mm; a somewhat flattening effect appears for our data but not at the same point. The slopes of the responses are

also different. These differences are not surprising considering the very different mechanics involved; in fact, it is the similarities that are surprising.

An argument could also be made that our data show an inverted U-shape response, only we could not create small enough groove widths to see the increasing leg of the curve. This is given credence by the significantly improved fit for a quadratic vs. linear response for the ridge width of 3.5 mm. The inverted U-shape is similar to previous data using regularly spaced dots (Conner and Johnson 1990) and jittered dots (Klatzky et al., 2003) with the bare finger and a hand held probe, respectively. However, the results from Klatzky et al. (2003), at least, are under very different conditions (i.e., a probe and jittered dots) compared to ours.

Finally, our results should be compared to that of Lawrence and his colleagues (2007) who extensively looked at square wave gratings, as did we, for both a bare finger and a probe. It should be noted that in their results, they obtained a very consistent form of the response whether a bare finger or probe was used (i.e., under very different mechanical conditions). However, our results appear to mirror theirs in that the flatter portion of the response is at small groove widths and the slope decreases with increasing groove width rather than increasing.

The mirroring of the results of Lawrence et al. (2007) may not be surprising when we consider the interaction between the fingerpad and the pins as compared to a physical grating. In studies with physical gratings, the finger's resting position is situated on a ridge, or at least on the level of the ridges (the grooves are etched into the plate or surface). It is the grooves which cause the deformation of the finger. In contrast, on our device the finger rests on the surface of the Braille cell, which constitutes the groove. The ridges are manifested by the raised pins, which actively deform the finger (see Figure 22 below). Thus in the present experiment, for a given ridge width, as the groove width is increased, the proportion of time during which the

finger is deformed decreases; conversely, at an increased ridge width, for any given groove width, the proportion of time the finger is deformed is increased, and the perceived roughness is higher.

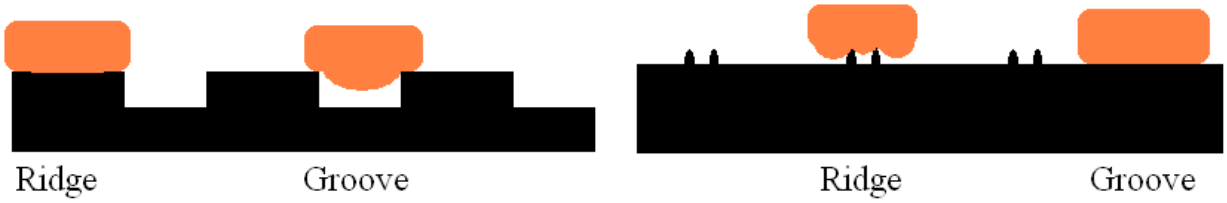

Figure 22. Finger deformation in the case of physical square-wave gratings (left) and virtual square-wave gratings rendered through a haptic matrix display (right).

Another difference between the results of this study and Lawrence et al.'s study is the fact that both ridge width and groove width were found to be significant factors – both at high levels of significance and effect size. Considering the reversal of roles of groove width and ridge width in the deformation of the finger discussed above, it is not surprising that ridge width is significant. The finding that groove width is also significant suggests that the amount of space and/or time in which the finger is not deformed also contributed (negatively) to the perception of roughness.

Finally, another interesting observation of the data is the significant difference in the perceived roughness when only one pin is used compared to eight pins. This has important implications for designing tactile diagrams in that creating a line or an area with a given texture will produce very different perceptual responses. It suggests that when using texture to describe multiple areas of a similar nature (e.g., arid conditions on a map) careful attention to the interaction between area size and texture is needed. However, the fact that the shape of the curve for the single pin response and the multiple pin response are very similar suggests that similar

mechanisms may be involved, from which we can conclude that the mechanisms are, at least in part, temporal in nature.

5.4 Experiment 2 – Ridge Width

Because ridge width was implicated as a significant factor contributing to roughness, and because we believed the ridges constituted the actively deforming stimuli in this experiment, Experiment 2 was conducted with the same protocol as above except that the stimuli consisted of 32 gratings produced from sixteen ridge widths crossed with two groove widths.

5.4.1 Methods

Participants

Fifteen (seven females, eight males; mean age = 33.4 years, SD = 13.9 years) participated in the experiment. Of the fifteen, two subjects were totally blind and four subjects were visually impaired. All but three subjects reported being right-handed (one indicated she was ambidextrous, but completed the experiment using her right hand only). Participants were divided into two groups: those who were sighted (9) and those that were visually impaired (6).

Apparatus and Stimuli

A set of 32 virtual vertical gratings were used as texture maps. The dimensions of the vertical gratings varied by ridge width (approximately 0.5 mm, 1 mm, 1.5 mm, 2 mm, 2.5 mm, 3 mm, 3.5 mm, 4 mm, 4.5 mm, 5.5 mm, 6.5 mm, 7.5 mm, 8.5 mm, 9.5 mm, 10.5 mm, 11.5 mm) and groove width (0.5 mm and 3.5 mm), with both dimensions completely crossed.

Procedure

The same procedure was used as for Experiment 1. The only difference between the studies was the variation in ridge width as opposed to groove width previously.

5.4.2 Results

The results are shown below in Figure 23. In all cases, roughness appears to be a quadratic function of ridge width. These quadratic trends were observed in all individual results. Consistent with the results of Experiment 1, larger roughness magnitudes were reported when groove width was held at 0.5 mm as compared to 3.5 mm. It is also clear that the single-pin condition yielded lower roughness magnitudes than the all-pin condition.

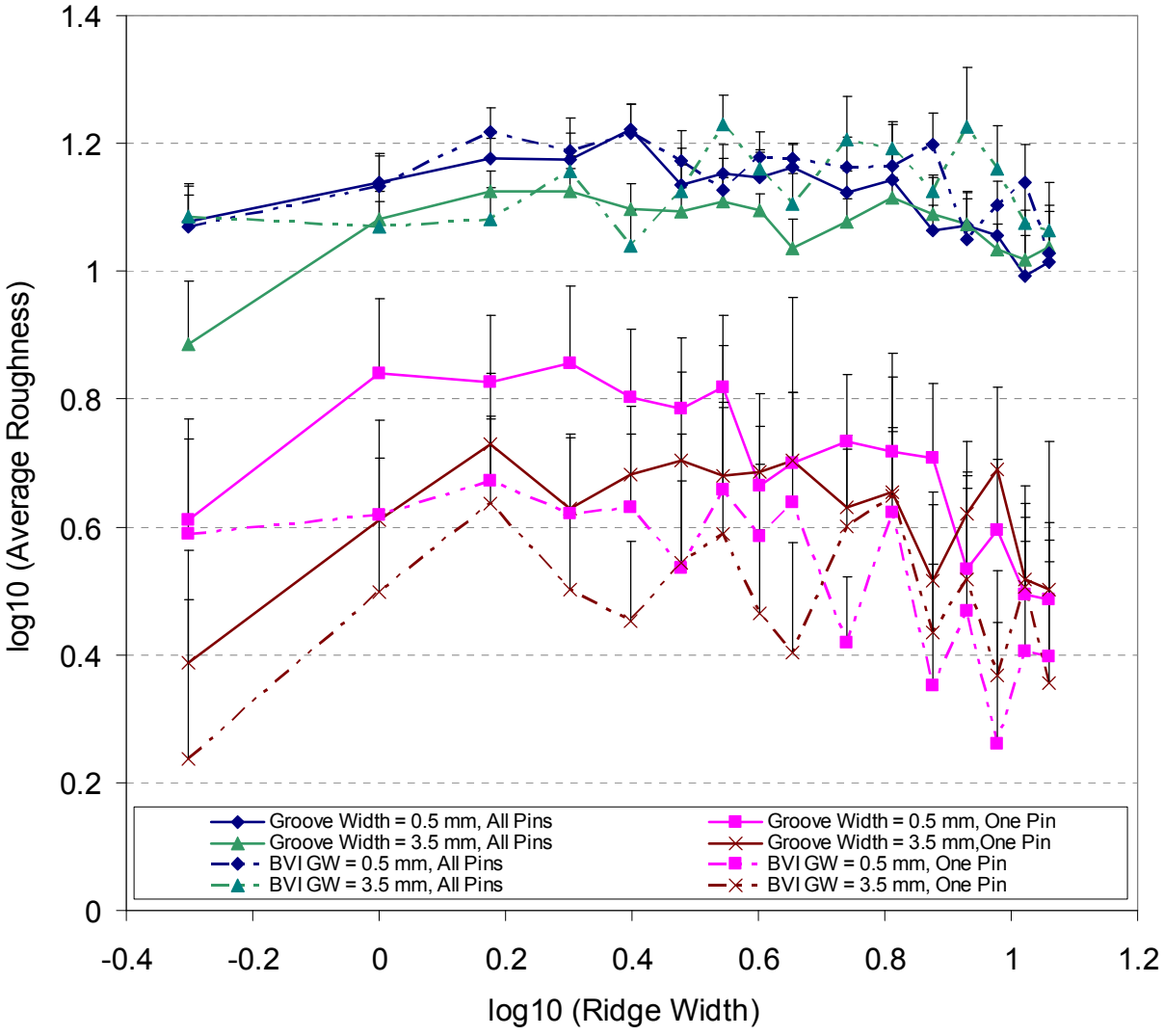

Figure 23. Experiment 2 results. Error bars indicate 1 SEM.

Linear and quadratic approximations were fit to each of the four obtained psychophysical functions (relating them to a power law). The R^2 values for these fits are provided in Table 3. In all cases, the quadratic fit was a dramatic improvement over the linear fit. The quadratic fits are shown in Appendix A in Figure A3. For the curve obtained with groove width = 0.5 mm and one pin activated, however, the R^2 value was still not very high.

Table 3. R^2 values for curve fits for the results of Experiment 2.

Groove Width	Number of Pins	Linear Fit R^2	Quadratic Fit R^2
0.5 mm	8	0.1753	0.8722
0.5 mm	1	0.4292	0.6073
3.5 mm	8	0.0921	0.9133
3.5 mm	1	0.0194	0.7349

Although the data for some individuals were noisy, most individuals generated curves similar in shape to the group means presented in Figure 23, with the exception of Subjects 8, 9 and 14, for whom the psychophysical functions obtained with all pins (but not with 1 pin) appear to be more strongly linear (in log-log space), and for Subject 10, for whom all psychophysical functions were linear (again, in log-log space).

Table 4. Significant ANOVA results for Experiment 2.

Effect	F	Significance	η^2
Number of pins	39.89	<.001	0.754
Ridge width	8.649	<.001	0.400
Groove width	1.777	0.021	0.344
Repetition * Ridge width * Vision	1.730	0.48	0.117
Repetition * Number of pins * Ridge width * Vision	2.514	0.002	0.162
Number of pins * Groove width * Ridge width * Vision	2.217	0.007	0.146

An ANOVA revealed significant main effects of number of pins ($F = 39.89$, $p < 0.001$, $\eta^2 = 0.754$), ridge width ($F = 8.649$, $p < 0.001$, $\eta^2 = 0.400$), and groove width ($F = 1.777$, $p = 0.021$, $\eta^2 = 0.344$) on the roughness perceived. Number of pins had a much larger effect size than ridge width or groove width, but their effect sizes were still significantly large. Vision or lack thereof was not found to be a significant factor. Despite this, three interaction effects, all including level of vision, were found to be significant (repetition * ridge width * vision, $F = 1.730$, $p = 0.48$, $\eta^2 = 0.117$; repetition * number of pins * ridge width * vision, $F = 2.514$, $p = 0.002$, $\eta^2 = 0.162$; number of pins * groove width * ridge width * vision, $F = 2.217$, $p = 0.007$, $\eta^2 = 0.146$). However, all of these interaction effects had small effect sizes, and so they were ignored.

5.4.3 Discussion

The present results surprisingly resemble the quadratic functions obtained by Connor and his colleagues (1990) for raised dot patterns felt with the finger and by Klatzky and her colleagues (Klatzky et al., 2003, Unger et al., 2010) for jittered raised dot patterns felt through both a physical and virtual probe. However, neither the spatial intensive model that can explain Connor et al.'s data (Taylor and Lederman 1975, Conner and Johnson 1992) nor the drop point model of Klatzky et al., (2003) are appropriate for a matrix device: the first cannot explain the results for a single pin, which is also quadratic, and the second is not appropriate for pins pushing into the skin.

It should be noted that although similar stimuli (i.e., square wave gratings) were used by Lawrence and his colleagues (2007), the responses were quite different between our experiments and theirs. This is still true even when we argue that the ridges in our experiment behave more like the grooves in their experiment in being the component that generates the biomechanical forces. They found roughness to increase with groove width and then plateau at higher widths.

Although similar to the left hand side of our figure, they have also argued that there is no right leg that decreases in response for higher groove widths as we have found for ridge width.

5.5 Experiment 3 – The Effect of Adaptation

5.5.1 Methods

Participants

Twelve subjects (seven females, five males; mean age = 37.8 years, SD = 15.5 years) participated in the experiment. Of the twelve, three subjects were totally blind and five subjects were visually impaired. All but one subject reported being right-handed. Participants were divided into two groups: those who were sighted (4) and those that were visually impaired (8).

Apparatus and Stimuli

The experiment was designed to compare the effect of adaptation between the tactile display, a bare finger and a probe. For the latter two, a set of nine physical vertical gratings spanning 50 mm in width were made out of 5.5" x 4.5" x 3/8" aluminum plates, using electrical discharge machining to achieve a groove depth of 0.45 mm, to serve as the stimuli to be explored. A corresponding set of nine virtual vertical gratings were also created to serve as the stimuli to be explored with the haptic device. The dimensions of the physical and virtual vertical gratings varied by ridge width and groove width; the dimensions are shown below in Table 5.

Table 5. Physical parameters of the square wave gratings used in Experiment 3.

Grating Number	Groove Width (mm)	Ridge Width (mm)
1	0.5	0.5
2	1.0	0.5
3	0.5	1.0
4	1.5	0.5
5	0.5	1.5
6	3.5	0.5
7	0.5	3.5
8	7.5	0.5
9	0.5	7.5

The stylus-like probes were machined from Delrin and were 121 mm long with a conical taper over the last 19 mm and ending in a sphere 1.5 mm in diameter.

The exploratory range was limited to 85 mm of horizontal movement and about 25 mm in vertical movement, in order to standardize the amount of exploration of textures and emphasize a side-to-side scanning exploratory procedure. For exploration with the device, a bounding box was assembled on the graphics tablet to limit the exploratory range of the device. For exploration with the probe and bare finger, a wooden frame was cut to hold the stimuli in place; a wooden cover was also constructed to rest on top of the grating. A rectangular window was milled into the wood to allow a probe or bare finger to access the grating below in a restricted exploratory range. The wall of the window closest to the subject was shaved down to an angle to allow a flatter finger contact with the grating. Pictures of the experimental setup for the device and for the probe and bare finger are shown below.

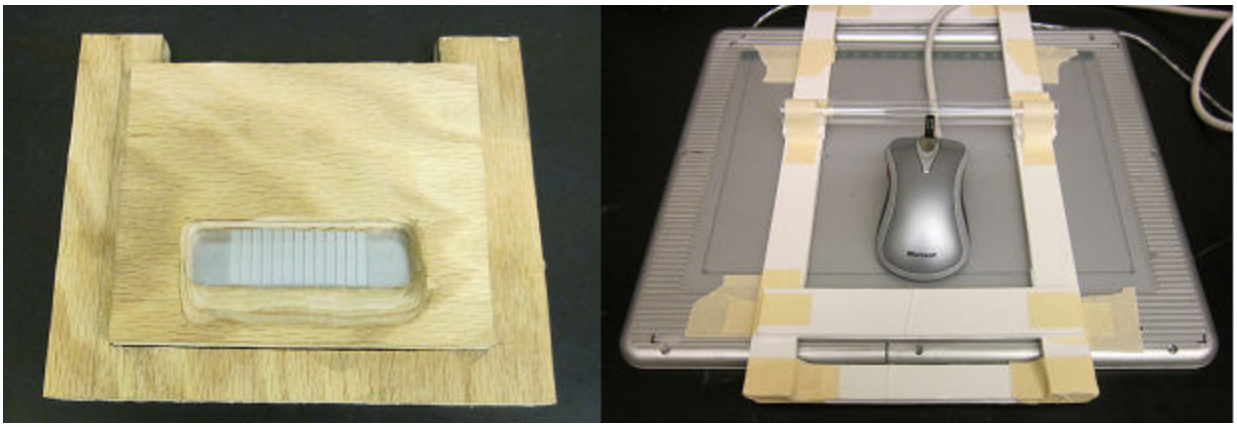

Figure 24. Bounding boxes for physical gratings (left) and virtual gratings (right) used in Experiment 3.

Procedure

The experiment consisted of three parts: exploration with the device, exploration with the probe, and exploration with the bare finger. For each mode of exploration, three different amounts of time of expose to an adapting stimulus were used: one minute, four minutes, or twelve minutes.

For each exposure time, either a smooth non-adapting surface or adapting surface was presented prior to each block. Six blocks of two repetitions of each of the nine gratings were presented to the subject for each mode of exploration, with a non-adapting and adapting stimulus for each adaptation time.

The non-adapting stimulus was actively explored for the same amount of time as the adapting stimulus. For the device, the non-adapting stimulus consisted of the Braille cell with no pins raised; thus the subject's finger rested on the casing of the Braille cell. For the probe and bare finger, the non-adapting stimulus consisted of the smooth unetched side of the metal gratings. Care was taken in the storage of the gratings to minimize any scratching to any face of the gratings. The physical adapting stimulus for exploration with a probe and the bare finger consisted of the grating with groove width equal to 1.5 mm and ridge width equal to 0.5 mm. This was chosen because it was the middle of the five gratings which varied in groove width (gratings 1, 2, 4, 6, and 8), and because groove width has been found to be the primary determinant of perceived roughness of metal gratings explored with the bare finger. The adapting stimulus for the device was the grating with groove width equal to 1.5 mm and ridge width equal to 0.5 mm, chosen to match the adapting stimulus of the probe and bare finger.

After the presentation of either the adapting or non-adapting stimulus of each block, subjects were presented with the two repetitions of the set of nine gratings in randomized order. Each of the eighteen trials consisted of a short period of exploration of the adapting or non-adapting stimulus (the same as was explored at the beginning of the block) for a duration of twenty seconds (as in Hollins et al., 2006). Subjects were asked to stop exploring at the end of the twenty seconds. The test grating was exchanged for the adapting or non-adapting grating, and the subjects were given seven seconds to explore the test grating (also as in Hollins et al.,

2006). At the end of the seven seconds, subjects rated the roughness of the gratings they had just explored using the absolute magnitude estimation method used in Experiments 1 and 2 described previously. Time was kept with a stopwatch.

In order to keep exploration speed with the device at or below 50 mm/s in order generate frequencies within the system bandwidth as discussing in Section 5.2, and to keep the exploration speed constant across the device, probe, and bare finger, a metronome was used to synchronize hand movements. An online metronome was first played through headphones in pilot work, but the interaction with other necessary programs caused the delivery of the sounds to be off-beat. A standalone, electronic metronome was used thereafter; the volume was sufficient to be heard through the headphones playing pink noise. The metronome was set to 40 beats per minute (bpm); participants were asked to explore with a speed of two beats per scan. Thus one beat coincided with the passing of the device, probe, or finger, through the middle of the stimuli, and one beat coincided with the arrival of the device, probe, or finger at the end of the exploratory range and the subsequent reversal of scanning direction. This value of 40 bpm kept exploration speed to less than 30 mm/s (85 mm x 40 bpm / 60 s / 2 scans). In pilot work, a setting of 60 bpm was initially used to limit the speed the 42.5 mm/s, but subjects were found to sometime increase their speed over 50 mm/s in order to compensate for getting off-beat, and so the value was decreased.

As in Experiments 1 and 2, subject wore a blindfold and headphones softly playing pink noise, loud enough to mask the sounds evoked during exploration, but soft enough to allow the metronome and experimenter's voice to be clearly heard.

5.5.2 Results

Two psychophysical functions were obtained from each of the three modes of exploration: one for a constant ridge width (gratings 1, 2, 4, 6, and 8) and one with groove width held constant (gratings 1, 3, 5, 7, and 9). These functions are plotted below in Figures 25, 26 and 27. The curves obtained for the device match those found in Experiments 1 and 2: a decreasing, primarily linear function in log-log space (although potentially quadratic) for constant ridge width, and an increasing slightly quadratic function for constant groove width. The drop-off at high ridge widths seen in Experiment 2 occurred after 7.5 mm and thus is not seen here.

More important to this experiment, however, was the presence and effect of adaptation on the perceived roughness of the gratings. In order to examine the effect of adaptation across adaptation times as well as across modes of exploration, the mean log perceived roughness was taken for all gratings, and then also for groups of gratings varying only in groove width or ridge width. For each adaptation time within each mode of exploration, the adapted mean was normalized to the null adapted mean. These values are shown below in Figure 28. The significance of the adaptation is indicated with an asterisk, as per the results of a t-test ($p < 0.05$).

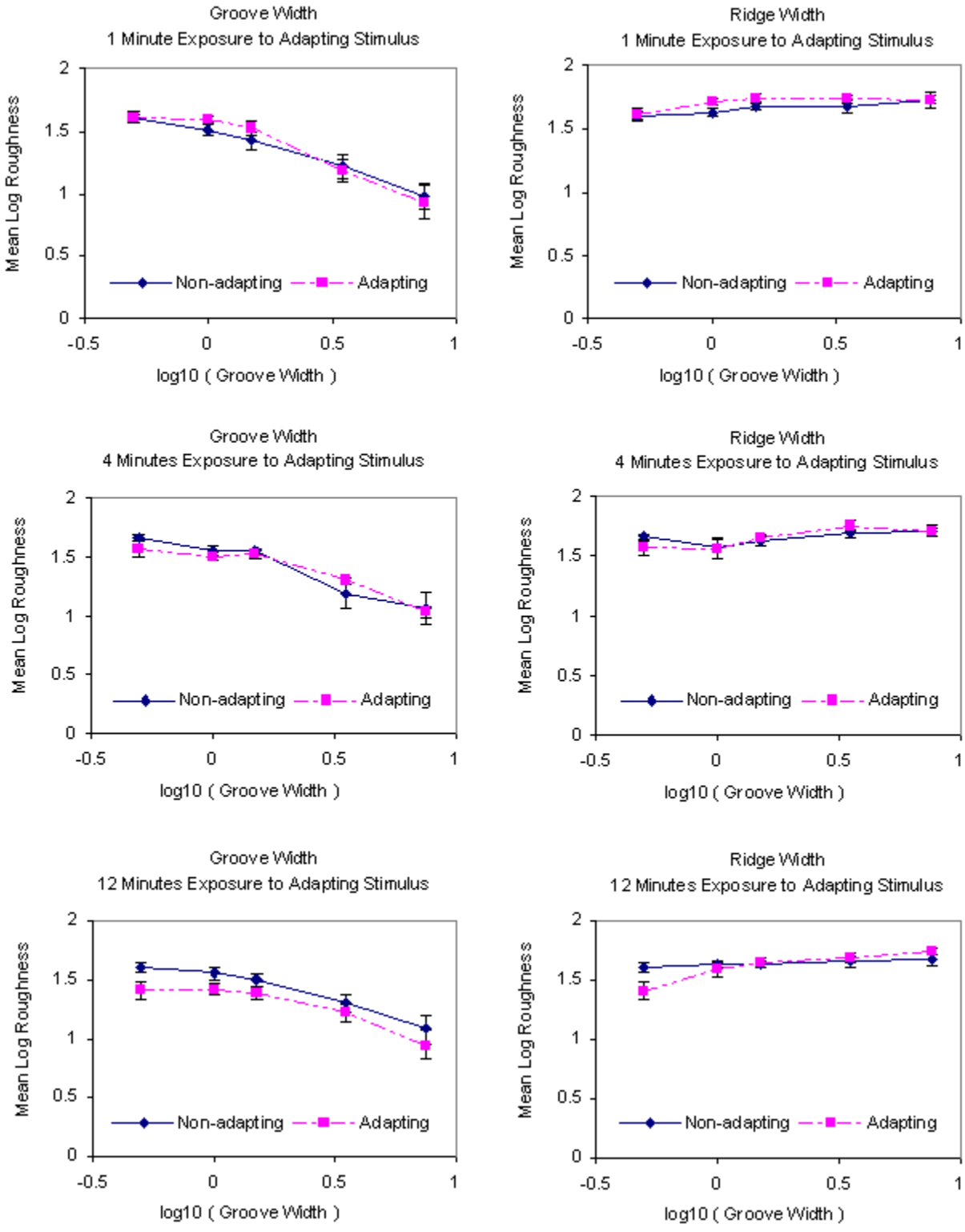

Figure 25. Experiment 3 results for exploration of gratings varying in groove width and ridge width for the matrix device, with exposure times of 1 minute, 4 minutes, and 12 minutes. Error bars indicate ± 1 SEM.

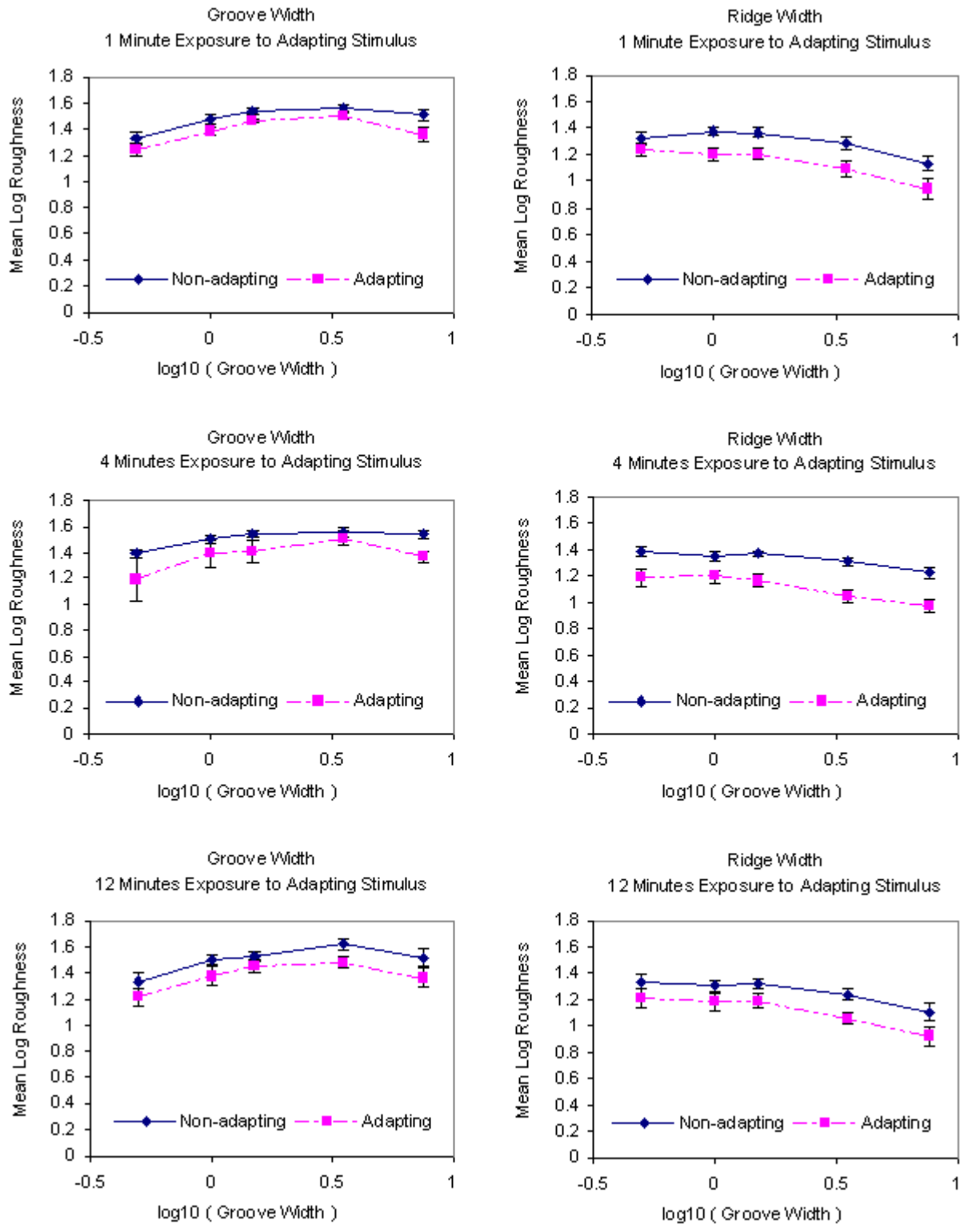

Figure 26. Experiment 3 results for exploration of gratings varying in groove width and ridge width for a handheld probe, with exposure times of 1 minute, 4 minutes, and 12 minutes. Error bars indicate ± 1 SEM.

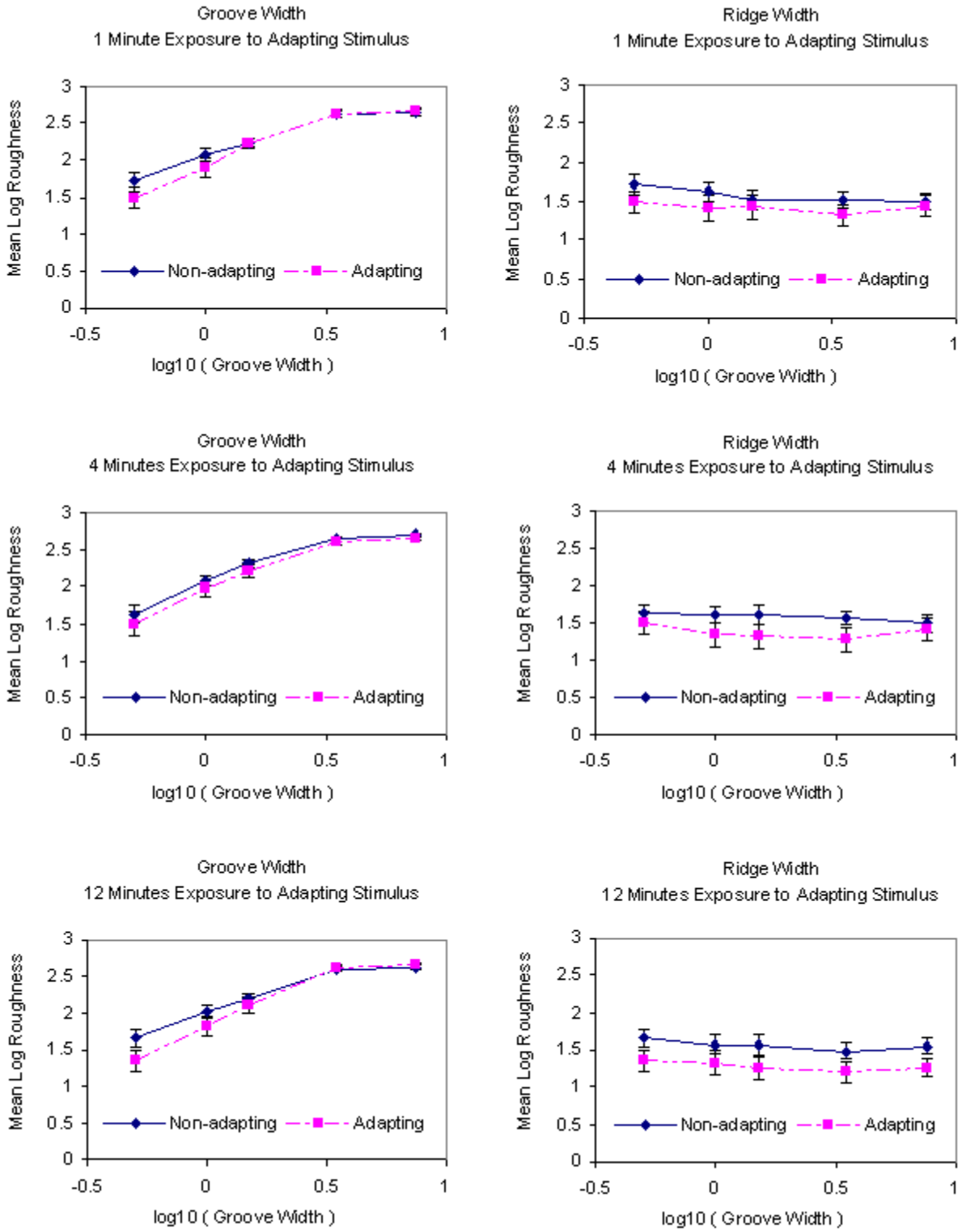

Figure 27. Experiment 3 results for exploration of gratings varying in groove width and ridge width for the bare finger, with exposure times of 1 minute, 4 minutes, and 12 minutes. Error bars indicate ± 1 SEM.

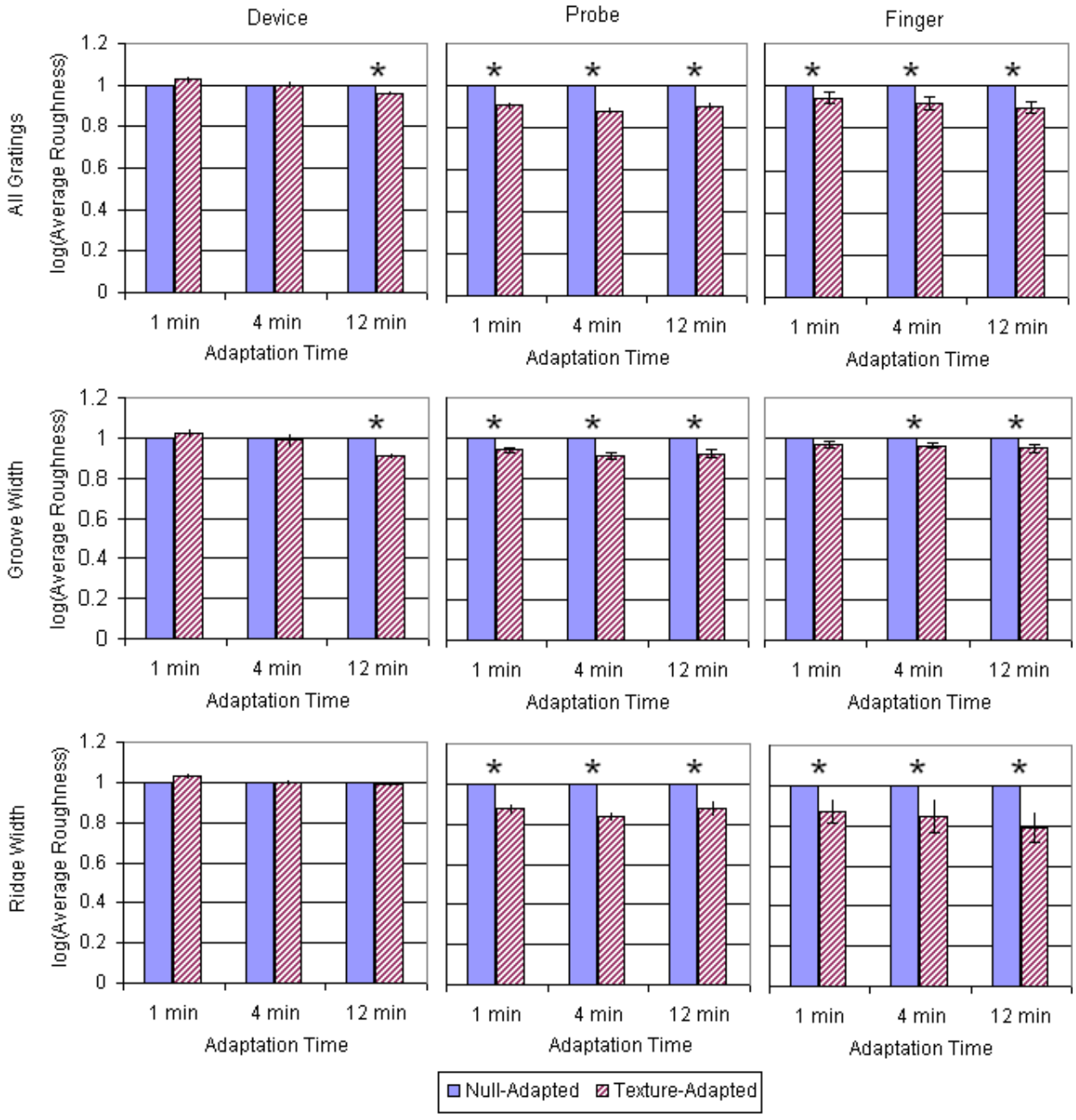

Figure 28. Averages of amount of adaptation across all gratings, those varying in groove width, and those varying in ridge width; for the device, probe, and finger. The asterisk indicates a significant difference between non-adapted and adapted averages.

Table 6. Significant ANOVA results for Experiment 3.

Effect	F	Significance	η^2
All Gratings			
Mode of exploration	16.993	<.001	0.630
Adaptation time	10.081	<.001	0.502
Vision * Mode of exploration	4.978	0.018	0.332
Gratings Varying in Groove Width			
Mode of exploration	5.345	0.014	0.348
Gratings Varying in Ridge Width			
Mode of exploration	12.398	<.001	0.554
Adaptation time	5.012	0.017	0.334
Vision * Mode of exploration	7.153	0.005	0.417
Vision * Adaptation time	3.650	0.045	0.267

An ANOVA of the individual means of all gratings for each adaptation time for all three modes of exploration revealed a significant effect of mode of exploration ($F = 16.993$, $p < 0.001$, $\eta^2 = 0.630$) and adaptation time ($F = 10.081$, $p < 0.001$, $\eta^2 = 0.502$). An interaction effect between being sighted or visually impaired and mode of exploration was observed ($F = 4.978$, $p = 0.018$, $\eta^2 = 0.332$), although being sighted or visually impaired was not significant itself ($F = 1.855$, $p = 0.203$, $\eta^2 = 0.157$).

An ANOVA of the individual means of gratings varying in groove width for each adaptation time for all three modes of exploration revealed a significant effect only of mode of exploration ($F = 5.345$, $p = 0.014$, $\eta^2 = 0.348$). Adaptation time was very close to being significant ($F = 10.081$, $p = 0.051$, $\eta^2 = 0.257$). No significant interaction effects were observed, and again, being sighted or visually impaired was not significant ($F = 0.070$, $p = 0.796$, $\eta^2 = 0.007$).

Finally, an ANOVA of the individual means of gratings varying in ridge width for each adaptation time for all three modes of exploration revealed a significant effect of mode of exploration ($F = 12.398$, $p < 0.001$, $\eta^2 = 0.554$) and adaptation time ($F = 5.012$, $p < 0.017$, $\eta^2 =$

0.334). An interaction effect between being sighted or visually impaired and mode of exploration was observed ($F = 7.153$, $p = 0.005$, $\eta^2 = 0.417$) as well as an interaction between being sighted or visually impaired and adaptation time ($F = 3.650$, $p = 0.045$, $\eta^2 = 0.267$). Being sighted or visually impaired was close to being significant ($F = 3.868$, $p = 0.078$, $\eta^2 = 0.279$).

ANOVAs were then carried out for each mode of exploration for all gratings, for gratings varying in groove width, and for gratings varying in ridge width, in order to determine the effects of adaptation within each mode of exploration. No significant effects were observed, but some were close to being significant. For the device, the effect of adaptation time was close to being significant for all gratings ($F = 3.292$, $p = 0.058$, $\eta^2 = 0.248$) and for gratings varying in groove width ($F = 3.299$, $p = 0.058$, $\eta^2 = 0.248$). Exploration with the bare finger yielded an almost significant effect of adaptation time only for gratings varying in ridge width ($F = 2.742$, $p = 0.089$, $\eta^2 = 0.215$). No effect close to significance was found for exploration with a handheld probe.

For these three effects, linear contrasts were found to be significant for all gratings with the device, ($F = 14.801$, $p = 0.003$, $\eta^2 = 0.597$); for varying groove width with the device, ($F = 16.366$, $p = 0.002$, $\eta^2 = 0.621$); for varying ridge widths explored with the bare finger, ($F = 5.222$, $p = 0.045$, $\eta^2 = 0.343$). Additionally, linear contrast for all gratings explored with the bare finger was close to significance ($F = 4.019$, $p = 0.073$, $\eta^2 = 0.287$). These contrasts indicate a trend for the conditions for which they are significant: as adaptation time increases, the amount of adaptation also increases.

Adaptation times were then fit to an exponential curve, assuming that the perception of roughness decayed exponentially. Since the adaptation times were not evenly spaced in time (60 s, 240 s, 720 s), the adaptation times for the overall mean of all the gratings, for the gratings

varying in groove width, and for the gratings varying in ridge width were fit to an exponential curve for all modes of exploration. The curve fits are shown in Appendix A in Figures A4, A5, and A6. The parameters are tabulated below.

Table 7. Parameters of Experiment 3 data fit to an exponential curve

Mode of exploration	Group	C	τ (s)	R^2
Haptic matrix display device	All	1.0302	10000	0.9821
	Groove Width	1.0312	5000	0.9986
	Ridge Width	1.0237	20000	0.7965
Handheld probe	All	0.8950	25000	0.0073
	Groove Width	0.9308	50000	0.1937
	Ridge Width	0.8553	33333	0.1465
Bare Finger	All	0.9418	14286	0.9322
	Groove Width	0.9700	33333	0.9986
	Ridge Width	0.8804	10000	0.9993

It can be seen that the adaptation time constant for gratings varying in ridge width explored with the bare finger is very similar to the time constant for gratings varying in groove width explored with the device. The results for the handheld probe were poorly fit with an exponential function as there was a "jump" between the null condition and the adaptation condition, with the adaptation condition remaining relatively constant across adaptation times.

5.5.3 Discussion

Because part of our experiment has similarities to previous experiments described in the literature, an agreement between the present results and those previously found would validate the experimental procedure. The psychophysical roughness functions found for the exploration of the stimuli varying in groove width with the bare finger match those found by Lawrence et al. (2007). The present data shows a very strong bipartite behavior, linearly increasing up to 3.5 mm groove width and then flattening out. As Lawrence and his colleagues did not examine ridge width in detail, they used more groove widths and found a slightly more quadratic function. The results from using a handheld probe likewise resemble the data found by Lawrence et al. Additionally, perceived roughness was not found to be any meaningful function of ridge width for gratings explored with the bare finger, as has been found in previous studies (e.g., Lederman 1974).

Although the results for exploration with a probe resemble those found by Lawrence et al., they employed a probe with a diameter of 3 mm, and speed was not controlled. In contrast, the present experiment used probes of 1.5 mm diameter, and speed was controlled. The drop point geometry explained by Klatzky et al. (2003) would predict the function peak to occur at 1.5 mm groove width, but the explanation put forth by Unger et al. (2010) explains the discrepancy: the velocity of the probe carries it over grooves into which it would otherwise fall completely; the effective drop point then increases. The occurrence of the function peak at a groove width larger than the diameter of the probe is thus in agreement with the literature. These overall similarities with the previous literature validate the experimental procedure and give credence to the results found for the haptic matrix display device, which also match well with the results found in Experiments 1 and 2.

The main objective, however, of Experiment 3 was to examine the effect of adaptation when textures are explored with the device as compared to adaptation effects seen with the bare finger and handheld probe. In terms of previous work, Hollins, Lorenz, and Harper (2006) examined adaptation to textures as opposed to vibrating stimuli, but used textures of a different nature and scale (2-D arrays of truncated pyramids varying in spatial period up to 1416 μm) than what we used (square-wave gratings varying in groove width and ridge width, with spatial periods ranging from 1 – 8 mm). They also only examined the effect of using a bare finger and a handheld probe. In comparing the only gratings that overlap between the two experiments, we found an effect of adaptation for both the probe and a bare finger, whereas Hollins et al. (2006) did not. In addition, whereas Hollins and his colleagues found the effect of adaptation on exploration with a probe to decrease as groove width (i.e., spatial period) increased, in the present results the trend shows the amount of adaptation remaining constant throughout the range of groove widths examined. Conversely, we found the effect of adaptation on exploration with the bare finger tending to decrease as groove width increased, whereas Hollins et al. found it to remain fairly constant as spatial period increased after 276 μm; in fact, for those larger spatial periods, the tendency is for a slightly higher response.

However, considering those spatial periods closest in frequency to ours (i.e., coarse textures between 276-944 um). Hollins et al. did find a significant difference between the adapted and null adapted mean perceived roughness for indirect touch (with a probe), but not direct touch (with the bare finger). We obtained similar results for gratings varying in groove width after one minute of adaptation (see Figure 28). However, when ridge width is varied, we have found it is the finger which encounters more adaptation.

There were several differences between our experiment and that of Hollins et al.: the tip diameter of their probe was 0.5mm, whereas ours was 1.5mm; they had participants stroke the textures in a circular motion, whereas we used side to side motion; the type of texture and the size of elements were different. These may explain some of the differences between the two experiments. However, one other difference that produced interesting results in our experiment was that we manipulated ridge width (akin to dot size). This parameter is not typically studied as it was found to have little effect on the perception of roughness with the bare finger (Lederman 1974; Lawrence et al., 2007). We included it as Experiment 1 and 2 suggested the importance of this parameter for perceiving roughness through our device. What was interesting, and surprising, was that although there was no visible trend of roughness being a function of ridge width, significant adaptation was found. This point will be discussed further in the Section 7.3 of the General Discussion below.

From Figure 28 it is evident that very little adaptation occurred when the device was used; significant adaptation was only found after twelve minutes of exploration of the adapting stimulus, for the average of all gratings and the average of all gratings varying in groove width (but not ridge width). Additionally, for the averages of all gratings and of those varying in groove width, linear contrast effects were found to be significant, indicating a trend of increasing adaptation as exposure time increases. These results show that the device, at least in response to the particular adapting stimuli used (see Section 7.1 below), is not very susceptible to adaptation; however, the effect will increase as exposure time increases.

In addition, for all three methods (the device, a handheld probe and a bare finger), we examined the effect of adaptation beyond the one minute time frame of Hollins and his colleagues. Our study examined the time course of adaptation, by using, additionally, four

minutes and twelve minutes of exposure time to the adapting stimuli. We found the effect of adaptation time to be significant. In the cases of exploration with the device and with the bare finger, a trend of increasing adaptation is evident as exposure time increases. The significant linear contrast effects support this trend.

Another interesting observation is that the amount and evolution of the adaptation time differed for gratings varying in groove width as opposed to those varying in ridge width. One aspect of particular interest, given our arguments in the discussion of Experiment 1 that the effects of grooves/ridges are reversed between using the bare finger and a matrix device, is that this reversal appears to occur for adaptation as well. This was true for whether the adaptation was or was not significant, which parameter could be explained by a linear contrast effect, and the time constants of the exponential decay. These matches make sense in light of the interaction between the fingerpad and the pins as compared to a physical grating described in the Discussion of Experiment 1. Taken together, this evidence suggests that exploration of virtual textures with a haptic matrix display is more like exploration of physical textures with the bare finger than with a handheld probe.

7. General Discussion

The current study has begun to address how virtual textures are perceived when generated on a haptic matrix device. As texture is one of the most effective dimensions perceived by touch, it is important to understand and take advantage of this dimension in effectively presenting tactile information. The experiments first focused on the effects of two stimuli components: the groove width and ridge width of square wave gratings. It also considered the area covered by the pins (i.e., number of pins) as we will want to vary this amount in real tactile presentations as well. All three parameters of the experiment strongly influenced the perceived magnitude of roughness. The third experiment examined the effect of texture adaptation on perception of texture through the matrix device, and compared it to texture adaptation when using a probe or the bare finger. The device was found to have the least amount of texture adaptation.

When examining the data, it is important to keep in mind the nature of the stimuli as displayed through the present haptic device. Because a Braille cell is used, there are only 8 pins which can deform the fingerpad as opposed to a continuous surface; therefore, only one of four spatial patterns was displayed at any given time (all pins down, all pins up, left column up / right column down, left column down / right column up). Furthermore, there was no tangential movement of the display with respect to the fingerpad, and, hence, also no friction. Thus, our results are in contrast to Smith et al. (2002) who found, for a similar range of spatial parameters, that the rate of variation in tangential stroking force is a significant determinant of roughness.

7.1 Study Limitations

Although this study was fairly extensive in investigating the effect of variation of parameters of groove width, ridge width, number of pins, and the effect of textures adaptation on exploration of

textures through a haptic matrix display as compared to exploration with a handheld probe and bare finger, only one type of texture, square wave gratings, was explored. This type of texture was chosen because of the similarities to previous work in the literature, but other types of stimuli have been used in the literature as well – most prominently (after square-wave gratings), 2-D arrays of dithered cones or truncated pyramids. As the 2-D structure of these textures makes them suitable for use in displaying 2-D tactile pictures, future studies with haptic matrix displays should examine the perceptual response to these stimuli as well.

Experiment 3 also used a single grating for the adapting stimulus, with the dimensions held constant across the modes of exploration. Although the choice of stimuli was based on the literature (Hollins et al., 2006) and holding it across modes of exploration provided consistency in the experimental protocol, the adapting stimuli as rendered through the device was perceived as being less rough than most of the other textures (Figure 25). In contrast, for the bare finger and probe, the adapting stimulus was judged to be one of the roughest textures. Thus, it is possible that the amount of adaptation when using the device would increase if the adapting stimulus used for the device was one of the rougher textures. With this comparative work completed, future studies will need to investigate whether different textures may cause more or less adaptation.

7.2 Implications for Texture Presentation through a Haptic Matrix Display

The results from all three experiments have implications for the design of textures presented through a haptic matrix display. The results of Experiment 1 show that groove width is a parameter which can be varied to change the perceived roughness of a texture. Although ridge width was found to be significant in both Experiments 1 and 2, the psychophysical function of Experiment 2 did not show as much change in roughness as ridge width was varied as was the

case when groove width was varied. In addition, the function was an inverted U-shape, with the two legs of the function producing the same texture perception. Thus, a smaller number of ridge widths should be used in creating different textures. Both Experiments 1 and 2 implicated contact area as a variable with a large effect on perceived roughness. These results can be applied to texture design in terms of the spatial layout of textures; textures covering larger areas will raise more pins on the display at a given time, and would be distinct from a texture covering smaller, narrower areas or lines that raised fewer pins. Finally, the results of Experiment 3 suggest that a haptic matrix display is not immediately susceptible to texture adaptation, supporting the use of textures in such a display. As adaptation is not known to be a problem in the exploration with the bare finger of actual tactile diagrams using texture, and less adaptation was found in this experiment with the device than with the bare finger, adaptation should not be an immediate concern for use of a matrix display to portray texture diagrams. However, the designer of textures is warned that adaptation was found to increase with increasing exposure time. The size and complexity of tactile pictures should not be so large or so difficult as to require the user to explore the picture for an extended period of time.

7.3 Potential Mechanisms of Sensation through a Haptic Matrix Display

In examining potential mechanisms for producing our response curves, we will first examine the case where only a single pin is moving (as a function of a square wave) on our matrix display. By the virtue of there being only a single pin, the temporal component must be what is important in conveying information about texture. For any conclusions drawn about the use of multiple pins, note that similarly shaped curves, both as a function of groove width and ridge width, were obtained for the single pin condition and the multiple pin condition.

For a single pin, as groove width is increased, the spacing between the square pulses increases. A receptor responding to constant indentation would generate impulses, the time trace of which would resemble the square wave. As a result the integration of the signal over time would decrease as the groove width increases. A receptor responding to the derivative of the deformation profile would respond less often as the groove width, essentially the time between indentations, increased. The integration of the response of such a receptor over time would also be a decreasing function of groove width. As the shapes of both of these integrations are decreasing functions of groove width, either or both of these signals could conceivably underlie the roughness functions gathered in Figure 21.

When ridge width is increased as groove width is held constant, the deformation profile changes to lengthen the contact with the finger pad. A receptor responding to constant indentation would emit impulses for longer periods of time as ridge width increases. The integration of that signal over time would be an increasing function of ridge width (although it may level off due to the refractory period of the receptor). The integration of the derivative of the movement profile would still decrease as ridge width was increased, since the edges would occur farther apart in space and time. The experimental data from the pilot study varying ridge width suggests roughness is a quadratic function of ridge width. We predict that the rise of the function at small ridge widths and the fall in the function at high ridge widths would require some combination of these integration functions.

The SA mechanoreceptors are known to respond proportionally to displacement as well as to the derivative of displacement. The RA mechanoreceptors also respond to the derivative of displacement. The present results indicate that activity of both of these mechanoreceptors or the SAs responding in both roles may be responsible for the present results.

The clear difference in the results of Experiments 1 and 2 between the use of multiple pins and a single pin strongly suggests that a spatial component is very important in the perception of roughness on matrix displays. However, this is not simply akin to using a real grating as the pins discretize the waveform. We will, though, consider a simple continuum mechanics model of the skin (Phillips and Johnson, 1981) when considering the effect of increasing the area of contact. What we would expect from such a model is that an increase in the contact area would increase the area of strain distribution in the skin, affecting the perceived response. However, as the pins are close together, this would not simply be an additive effect as their adjacency would lessen the strain between them. As expected, the response for multiple (8) pins is much greater than for a single pin but not a factor of eight times greater.

The results from Experiment 3 also shed some light on the possible mechanisms of perception through a haptic matrix display. Perception of textures through a probe is thought to be mediated primarily through the Pacinian channel (Yoshioka et al., 2007). For exploration with the bare finger, many studies have implicated the SA I channel as the primary mediator of the sensation of roughness. Supporting this, the time course of adaptation of the channels mediating the perception of roughness through the probe and the bare finger were found to be different in the results of Experiment 3. When exploring with a probe, the reduction in perceived roughness changed at a different rate as a function of exposure to the adapting stimulus as compared with the bare finger. However, it should be noted that these differences could be due to central mechanisms of the nervous system as well.

What is very interesting in our study is that the time course of adaptation is very similar between the matrix display device and the bare finger, but not the probe. Although the amount of adaptation appears to be less in the case of exploration with the matrix display, the rates of

change in adaptation as exposure time to the adapting stimulus increases are very similar. The difference could be that, although the physical parameters of groove width and ridge width are identical, the presentation through a physical grating could potentially be a stronger stimulus than the presentation through the device (as described earlier), and thus cause greater adaptation. Therefore, it seems that perception through a haptic matrix display device is more similar to exploration with the bare finger than through a probe.

The fact that adaptation was found as gratings varying in ridge width were explored with the bare finger but much less with groove width has implications for the possible mechanisms involved. Due to the similar but reverse effect with the matrix display (groove width had a greater effect than ridge width), it also has implications for the display. We will first examine the case of exploration with the bare finger. When the bare finger moves over square wave gratings varying in groove width, with ridge width held constant, no difference is perceived by the finger scanning the smooth surface of the grating until the first groove is encountered; it is the groove which actively deforms the finger. As the groove width increases, the deformation of the finger increases – this is a changing spatial pattern. (Although it should be noted that the frequency of deformations decreases.) This deformation is widely thought to be mediated by the SA I channel.

In the case of varying ridge widths with groove width held constant, however, the amount of deformation experienced per groove does not change. Instead, the frequency of such deformation changes – this is a changing temporal pattern. (Although an alternating spatial pattern is formed as well.) Although the perception of gratings varying in ridge width likely depends on the spatial component of the texture, it may also depend on this temporal component, to a larger degree than the perception of gratings varying in groove width.

Hollins et al. (2006) have posited that both spatial and vibrotactile (i.e., temporal) sensory codes are available in the exploration of coarse surfaces, but it is the spatial code that normally dominates. They hypothesized that extended exposure to adapting surfaces would decrease the tactile sensitivity to temporal cues, making the perception of roughness increasingly dependent on spatial cues. The evidence found in Experiment 3 of the diminished perceived roughness over time of gratings varying in ridge width (likely temporal cues), especially as compared to the lesser amount of adaptation found for gratings varying in groove width (likely spatial cues), supports this hypothesis as this likely shows the adaptation of sensory channels contributing to the perception of roughness based on temporal cues. This in turn implicates both the SA I and either the FAI or Pacinian channels, or both, in the perception of roughness of square-wave gratings when explored by the bare finger.

By virtue of the similarities between physical ridges and virtual grooves as displayed on a haptic matrix display, and between physical grooves and virtual ridges, these implications extend to the perception of gratings varying in groove width on a matrix display device. For virtual square wave gratings varying in groove width with constant ridge width, the actively deforming portion (the ridge, rendered by pin indentation) does not change in magnitude, only frequency. Conversely, when ridge width is varied, the magnitude of the actively deforming stimuli increases. The effect of adaptation seen for gratings varying in groove width, but not ridge width, when explored with a matrix display support this hypothesis, and likewise implicate both a spatial and temporal code in the perception of texture through a haptic matrix display. The SA I and either the FAI or Pacinian channels, or both, are thus implicated in this perception.

Finally, the lack of difference found between the performance of blind or visually impaired participants and sighted participants (consistent with Kornbrot et al. (2007) and Heller

(1989)) suggests that the application of the device may be extendable to areas outside of assistive technology. More importantly, however, this affirms that the burden of testing the device and supporting software in various stages of development need not fall solely on the shoulders of blind and visually impaired persons. They are still, of course, the most important assessors of the technology that is primarily aimed at their use.

8. Conclusion

Dynamic, refreshable tactile displays offer a method of displaying graphical information to people who are blind or visually impaired. Furthermore, texture is already used as an effective method to present graphical information in physical tactile diagrams, and would conceivably constitute the best way to present graphics through a tactile display. Although many such displays have been designed, very few low-cost systems have been conceived. This thesis has presented the design of a revised low-cost haptic matrix display device capable of displaying graphical information through virtual textures. New software and hardware increased the device's ability to display more diverse textures as compared to previous versions by adding the capability to display four amplitude levels and many accurate frequencies up to 125 Hz. The combination of possible amplitudes, frequencies, and spatial patterns of these two parameters give rise to a myriad of possible textures that can be displayed.

In order to limit this large set of textures to a more manageable set of salient and distinct textures useful for the portrayal of graphical information, and to determine how such textures are perceived through a haptic matrix display, three experiments were conducted. The first and second examined the perception of roughness of square wave gratings varying in groove width, ridge width, and area of contact; the third focused on the effect of texture adaptation on perception through the device as compared to a handheld probe and the bare finger. The results of the first two experiments show that groove width and ridge width are effective parameters which may be changed to create textures of varying roughness. Contact area was also found to significantly contribute to the perception of roughness, so care must be taken as individual components of textures are created – different sized elements may be perceived differently. Finally, the results of the third experiment suggest that exploration with a matrix display device

is not as susceptible to texture adaptation as are exploration with a probe or the bare finger; however, with increased exposure time adaptation can occur. It is believed that these results are applicable to other haptic matrix display systems and thus will aid in the development of more effective methods of displaying graphical information through the human haptic system.

References

[1] Alary, F., Duquette, M., Goldstein, R. Chapman, C.E., Voss, P., La Buissonniere-Ariza, V. and Leopore, F. (2009). Tactile acuity in the blind: A closer look reveals superiority over the sighted in some but not all cutaneous tasks. Neuorphysiologica, 47, 2037-2043.

[2] Bensmaia, S., and Hollins, M. (2003). The vibrations of texture. Somatosensory Motor Research, 20 (1), 33-43.

[3] Bliss, J., Katcher, M., Rogers, C., and Shepard, R. (1970). Optical-to-Tactile Image Conversion for the Blind. IEEE Transactions on Man-Machine Systems, 11 (1), 58-65.

[4] Chan, J., Maucher, T., Schemmel, J., Kilroy, D., Newell, F., and Meier, K. (2007). The virtual haptic display: A device for exploring 2-D virtual shapes in the tactile modality. Behavior Research Methods, 39 (4), 802-810.

[5] Connor, C., Hsiao, S., Phillips, J. and Johnson, K. (1990). Tactile roughness: Neural Codes That Account for Psychophysical Magnitude Estimates. The Journal of Neuroscience, 10 (12), 3823-3836.

[6] Connor, C., Johnson, K. (1992). Neural coding of tactile texture: comparison of spatial and temporal mechanisms for roughness perception. The Journal of Neuroscience, 12 (9), 3414-3426.

[7] Craig J. (1977). Vibrotactile Pattern Perception: Extraordinary Observers. Science, 196 (4288), 450-452.

[8] Gescheider, G., Wright, J., and Verrillo, R. (2009). Information-Processing Channels in the Tactile Sensory System: A Psychophysical and Physiological Analysis. Psychology Press, New York, NY.

[9] Headley, P. and Pawluk, D. (2010). A Low-Cost, Variable Amplitude Haptic Distributed Display for Persons who are Blind and Visually Impaired. ACM Assets, Orlando, Florida, October 25-27.

[10] Heller, M. (1989). Texture perception in sighted and blind observers. Perception and Psychophysics, 45 (1), 49-54.

[11] Hollins, M., Bensmaia, S., Washburn, S. (2001). Vibrotactile adaptation impairs discrimination of fine, but not coarse, textures. Somatosensory & Motor Research, 18 (4), 253-262.

[12] Hollins, M., Faldowski, R., Rao, S., and Young, F. (1993). Perceptual dimensions of tactile surface texture: A multidimensional scaling analysis. Perception & Psychophysics, 54 (6), 697-705.

[13] Hollins, M., Lorenz, F., and Harper, D. (2006). Somatosensory Coding of Roughness: The Effect of Texture Adaptation in Direct and Indirect Touch. The Journal of Neuroscience, 26 (20), 5582-5588.

[14] Hollins, M., and Risner, S. (2000). Evidence for the duplex theory of tactile perception. Perception & Psychophysics, 62 (4), 695-705.

[15] Klatzky, R., Lederman, S., Hamilton, C., Grindley, M. and Swendsen, R. (2003). Feeling textures through a probe: effects of probe and surface geometry and exploratory factors. Perception and Psychophysics, 65 (4), 613-631.

[16] Kornbrot, D., Penn, P., Petrie, H., Furner, S. and A. Hardwick (2007). Roughness perception in haptic virtual reality for sighted and blind people. Perception and Psychophysics, 69 (4), 502-512.

[17] Lawrence, M., Kitada, R., Klatzky, R. and Lederman, S. (2007). Haptic roughness perception of linear gratings via bare finger or rigid probe. Perception, 36, 547-557.
[18] Lederman, S. (1974). Tactile roughness of grooved surfaces: the touching process and effects of macro- and microsurface structure. Perception and Psychophysics, 16 (2), 385-395.
[19] Lederman, S. (1981). The perception of surface roughness by active and passive touch. Bulletin of the Psychonomic Society, 18, 253-255.
[20] Lederman, S., Klatzky, R., Hamilton, C. and Grindley, M. (2000). Perceiving surface roughness through a probe: effects of applied force and probe diameter. Proceedings of the ASME Dynamic Systems and Control Division, 69-2, 1065-1071.
[21] Lederman, S., Loomis, J., and Williams, D. (1982). The role of vibration in the tactual perception of roughness. Perception & Psychophysics, 32 (2), 109-116.
[22] Levesque, M. (2005). Blindness, Technology, and Haptics. Technical Report TR-CIM-05.08. McGill University, Canada.
[23] Levesque, V. and Hayward, V. (2008). Tactile graphics rendering using three laterotactile drawing primitives. Proceedings of the 16th Symposium on Haptic Interfaces for Virtual Environment and Teleoperator Systems, March 13-14, Reno, Nevada, 429-436.
[24] Linvill, J., and Bliss, J. (1966). A Direct Translation Reading Aid for the Blind. Proceedings of the IEEE, 54 (1), 40-51.
[25] Loomis, J., Klatzky, R., and Lederman, S. (1991). Similarity of tactual and visual picture recognition with limited field of view. Perception, 20, 167-177.
[26] Jones, L., and Lederman, S. (2006). Human Hand Function. Oxford University Press, New York, NY.
[27] Owen, J., Petro, J., D'Souza, S., Rastogi, R., and Pawluk, D. (2009). An Improved, Low-cost Tactile "Mouse" for Use by Individuals Who are Blind and Visually Impaired. ACM Assets, Pittsburg, Pennsylvania, October 25-28.
[28] Phillips, J. and Johnson, K. (1981) Tactile Spatial Resolution. III. A Continuum Mechanics Model of Skin Predicting Mechanoreceptor Responses to Bars, Edges and Gratings. Journal of Neurophysiology, 46 (6): 1204-1225.
[29] Rastogi, R., Pawluk, D., and Ketchum, J. (2010). Issues of Using Tactile Mice by Individuals Who Are Blind and Visually Impaired. IEEE Transactions on Neural Systems and Rehabilitation Engineering, 18 (3), 311-318.
[30] Rovira, K., Gapenne, O., and Ammar, A. (2010). Learning to recognize shapes with a sensory substitution system: a longitudinal study with 4 non-sighted adolescents. 2010 IEEE 9th International Conference on Development and Learning, 1-6.
[31] Smith, A, Chapman, C., M. Deslandes, J-S. Langlais, M-P. Thibodeau. (2002). Role of friction and tangential force variation in the subjective scaling of tactile roughness. Experimental Brain Research, 144, 211-223.
[32] Taylor, M. and Lederman, S. (1975). Tactile roughness of grooved surfaces: A model and the effect of friction. Perception and Psychophysics, 1975, 17 (1), 23-36.
[33] Thomas, P., Isabelle, P., Benoit, M. (2006). Static and dynamic directional cues experiments with VTPlayer mouse. Eurohaptics 2006, Paris, France, 63-68.
[34] Thompson, L., Chronicle, E., and Collins, A. (2006). Enhancing 2-D Tactile Picture Design from Knowledge of 3-D Haptic Object Recognition. European Psychologist, 11 (2), 110-118.

[35] Unger, B., Hollis, R. and Klatzky, R. (2010). Roughness Perception in Virtual Textures. To Appear in the IEEE Transactions on Haptics.
[36] Van Erp, J. (2002). Guidelines for the Use of Vibro-Tactile Displays in Human Computer Interaction. Eurohaptics 2002.
[37] Vidal-Verdu, F., and Hafez, M., (2007). Graphical Tactile Displays for Visually-Impaired People. IEEE Transactions on Neural Systems and Rehabilitation Engineering, 15 (1), 119-130.
[38] Wall, S., and Brewster, S. (2006). Sensory Substitution using tactile pin arrays: Human factors, technology and application. Signal Processing, 86, 3674-3695.
[39] Wall, S. and Harwin, W. (2001). Interaction of visual and haptic information simulated environments: texture perception. In S. Brewster and R. Murray-Smith (Eds.) Haptic human-computer interaction, Springer, Berlin, 108-117.
[40] Yoshioka, T., Bensmaia, S., Craig, J., Hsiao, S. (2007). Texture perception through direct and indirect touch: An analysis of perceptual space for tactile textures in two modes of exploration. Somatosensory and Motor Research, 24 (1-2), 53-70.
[41] Zwislocki, J.J., and Goodman, D.A. (1980). "Absolute scaling of sensory magnitudes: A validation." Perception & Psychophysics 28 (1): 28-38.

Appendix A

Curve fits for Experiments 1, 2, and 3

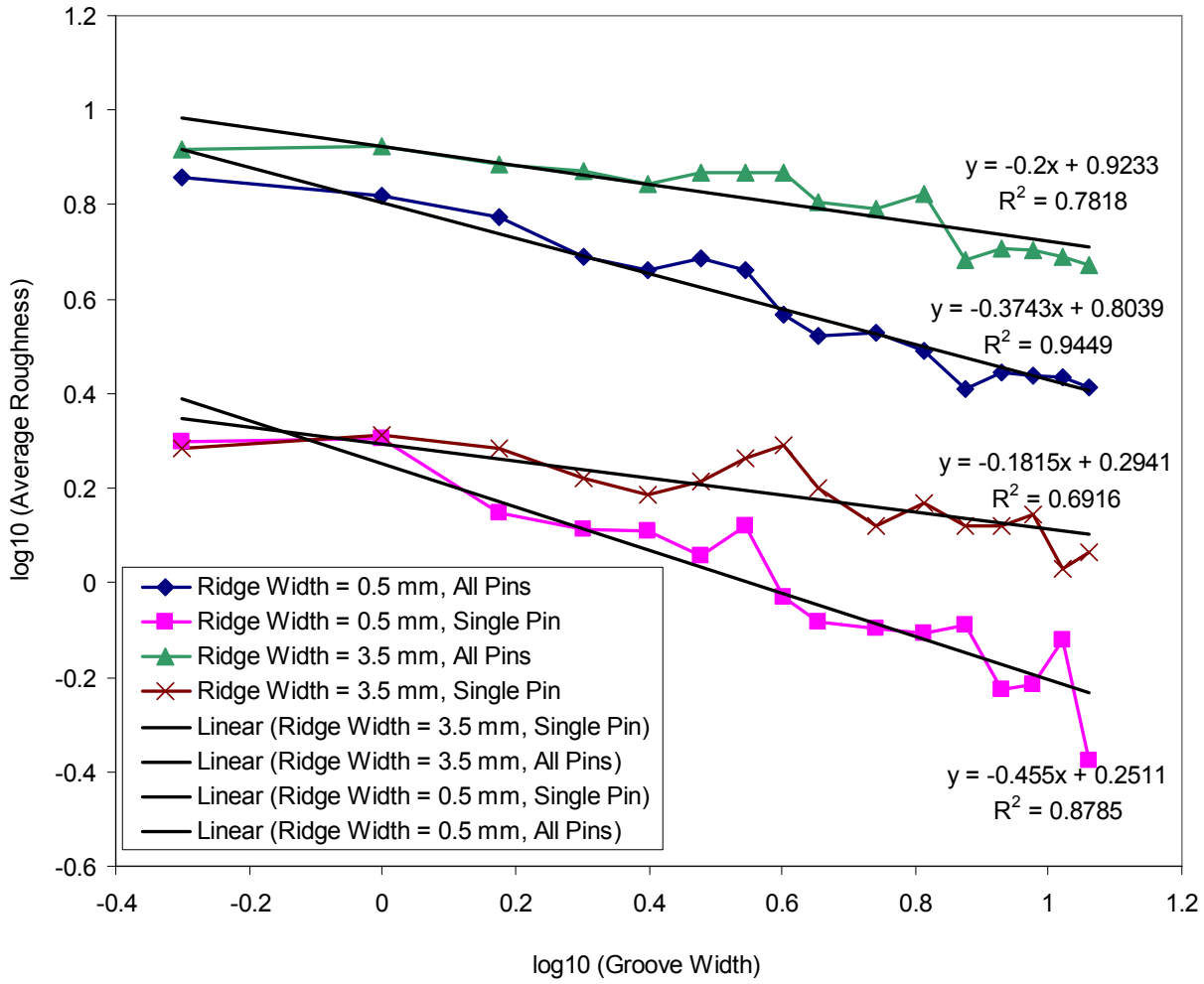

Figure A1. Linear curve fits for the results of Experiment 1.

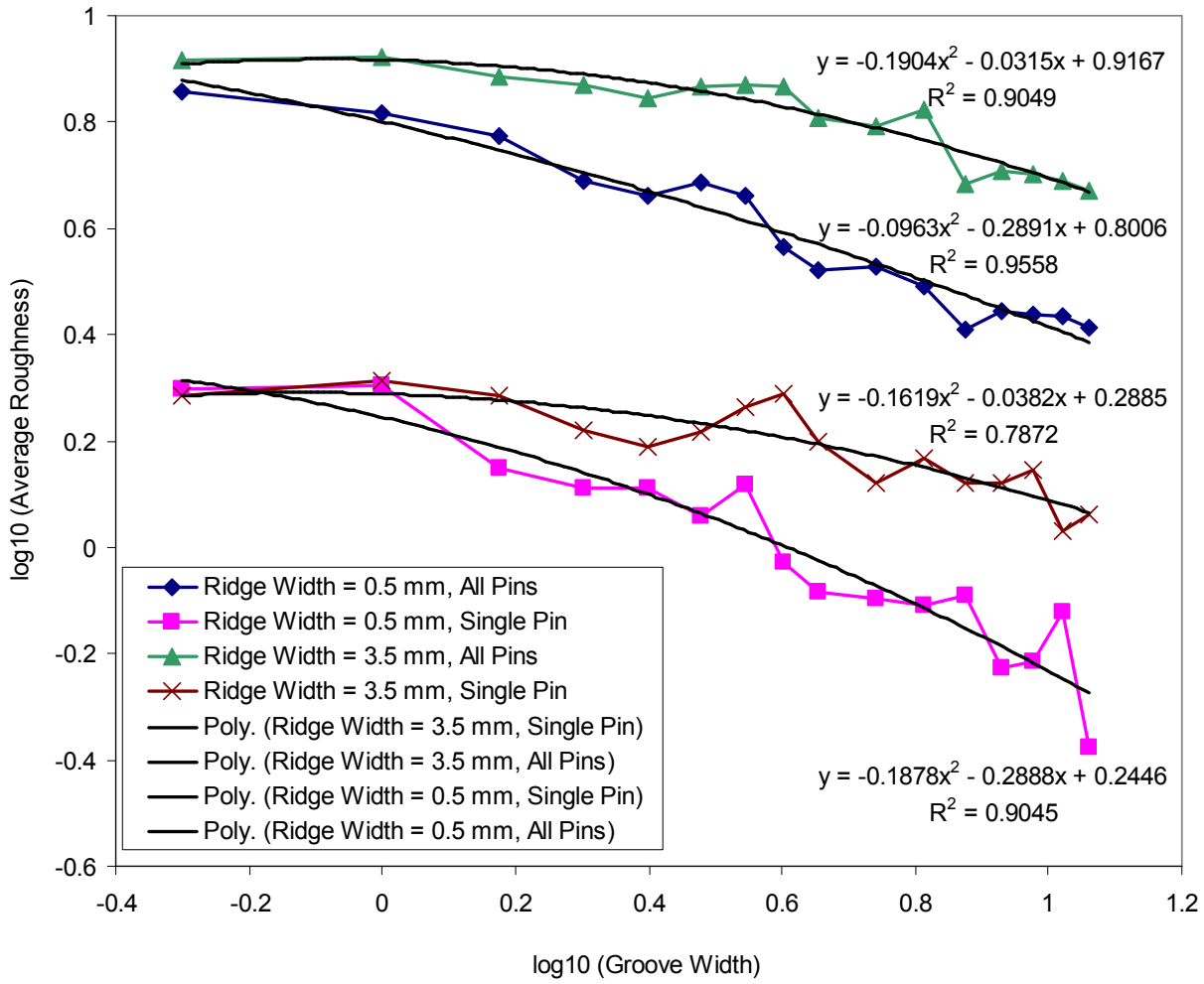

Figure A2. Quadratic curve fits for the results of Experiment 1.

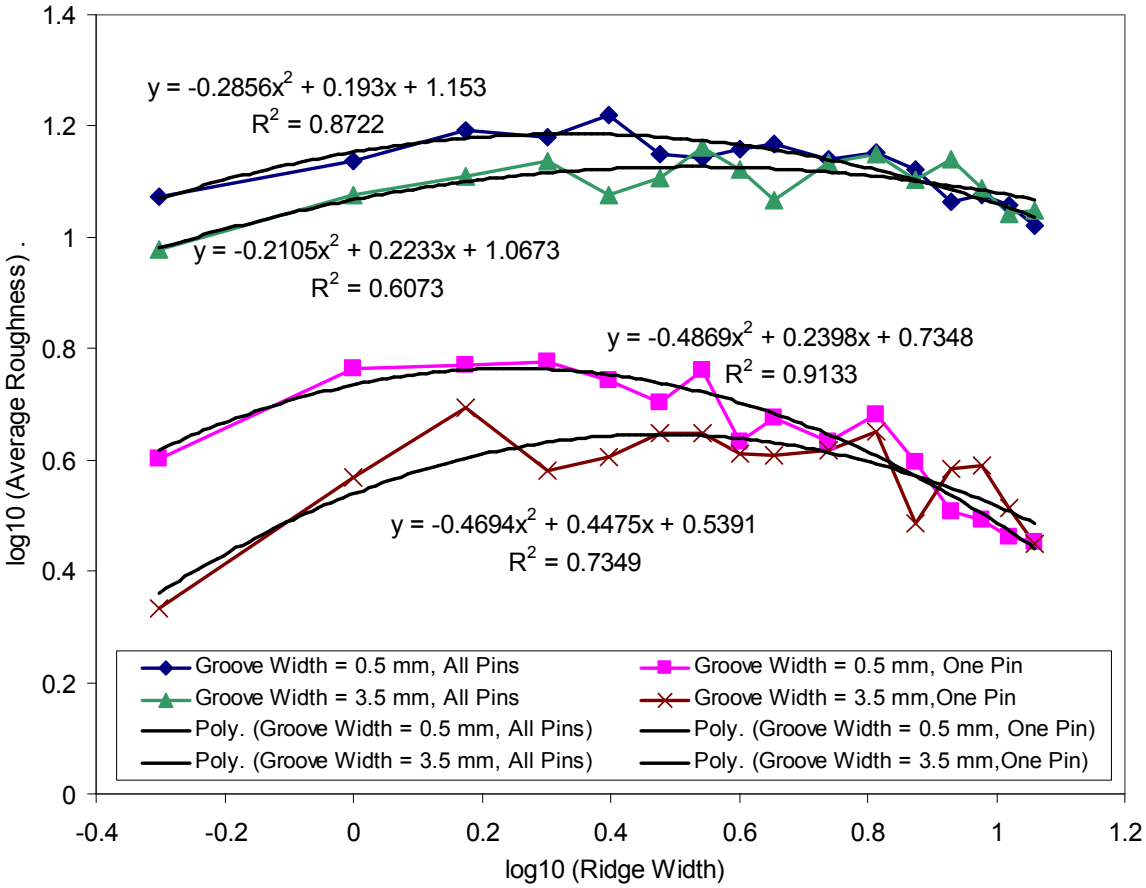

Figure A3. Quadratic curve fits for the results of Experiment 2.

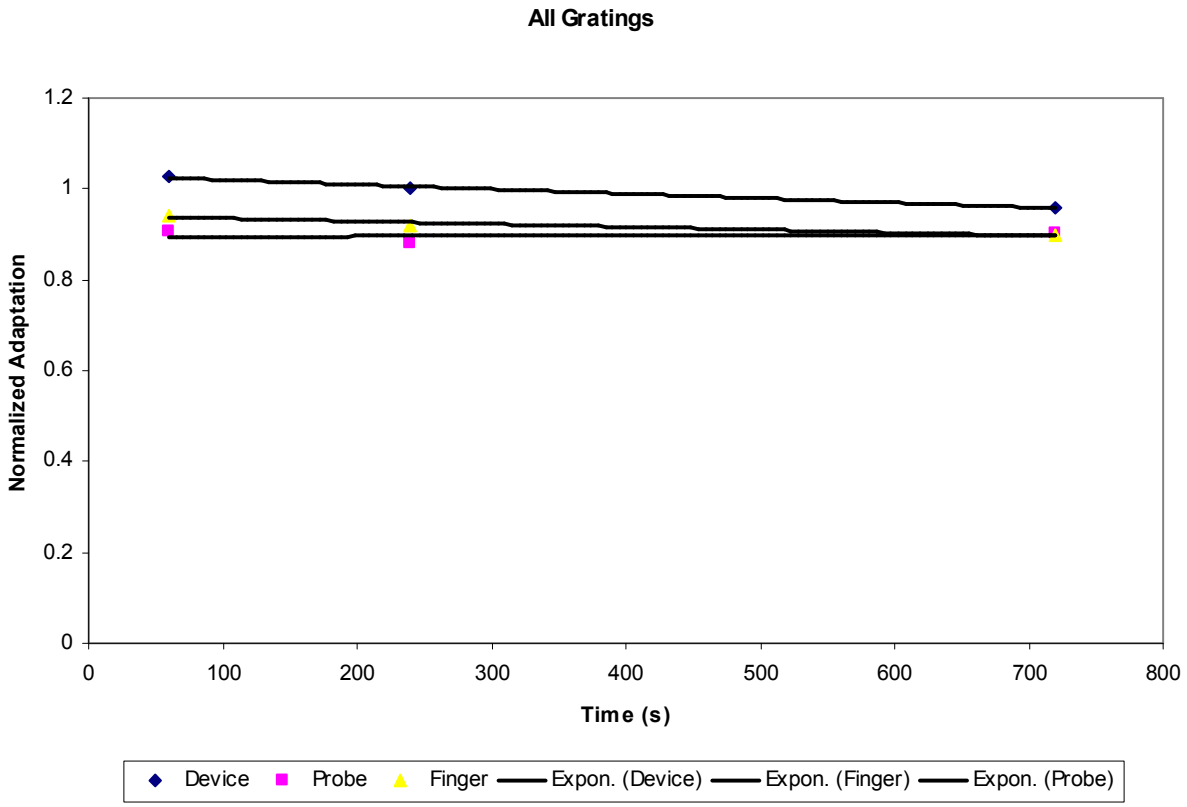

Figure A4. Exponential curve fits for the averages of all gratings from Experiment 3.

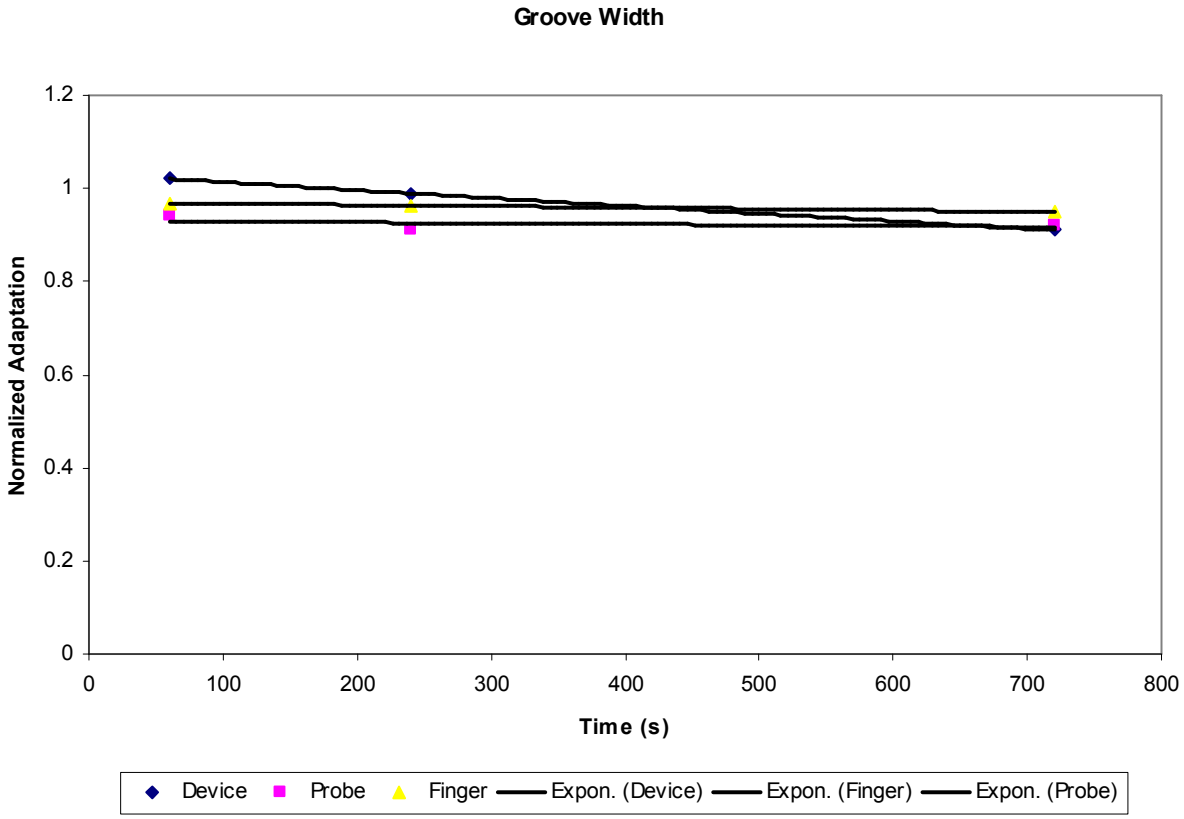

Figure A5. Exponential curve fits for the averages of the gratings varying in groove width from Experiment 3.

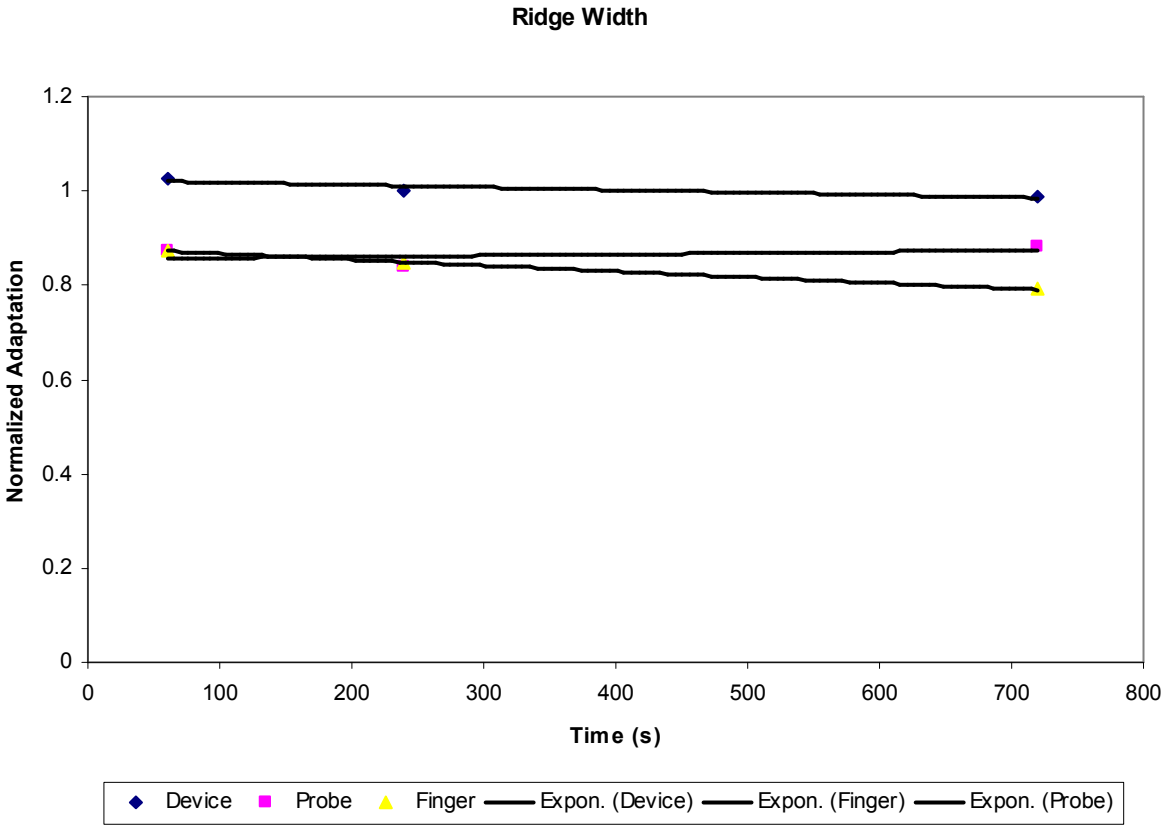

Figure A6. Exponential curve fits for the averages of the gratings varying in ridge width from Experiment 3.